Solvation and Dynamics of CO_2 in Aqueous Alkanolamine Solutions

Sergey M. Melnikov[1], *Matthias Stein*[1 *]

[1]Molecular Simulations and Design Group, Max Planck Institute for Dynamics of Complex Technical Systems, Sandtorstrasse 1, 39106 Magdeburg, Germany.

*Corresponding author: Dr. Matthias Stein, phone +49-391-6110436, matthias.stein@mpi-magdeburg.mpg.de

Keywords: diffusion, sequestration, biogas upgrading, computer-aided molecular design, molecular dynamics

Abstract

Carbon dioxide sequestration from flue gases by chemical absorption is the most versatile process. The molecular engineering of novel high-performant biogas upgrading alkanolamine compounds requires detailed information about their properties in mixed solution. The liquid structure properties of four representative alkanolamine molecules (monoethanolamine (MEA) as a reference and standard, 3-aminopropanol (MPA), 2-methylaminoethanol (MMEA) and 4-diethylamino-2-butanol (DEAB)) in the presence of CO_2 were investigated over a wide range of solvent alkanolamine/water mixture compositions and temperature. In aqueous solution, for the alkanolamine molecules MEA, MPA and MMEA hydrogen bonding with solvent water molecules is dominating over CO_2 interactions. Analysis of the liquid structure reveals that carbon dioxide shows no preference of approaching the alkanolamine but is rather displaced by water molecules as the water content increases. CO_2 dissolved in aqueous DEAB, however, accumulates within clusters of DEAB molecules almost devoid of water. The calculated carbon dioxide diffusion coefficients for all four molecules agree well with experiment where available and are obtained for all mixture compositions and as a function of temperature. The solute diffusion correlates with the mobility of the alkanolamines in water at various ternary mixture compositions. Kinetic aspects of the CO_2-alkanolamine interactions are described by characteristic residence times of CO_2. The hydrophobic interaction of carbon dioxide with the alkanolamine has a lifetime of the order of tens of picoseconds whereas polar interactions are about one order of magnitude shorter. The tertiary amine DEAB displays many favorable features for an efficient CO_2 chemisorption process. Molecular engineering of novel compounds for absorptive sequestration has to take into account not only the thermodynamics and chemical reactivity but also liquid structure properties, the dynamics of CO_2 diffusion and the kinetics of interactions in complex ternary solutions.

Introduction

Global energy consumption and demand are continuously increasing but the majority of the resources exploited like petroleum, natural gas, and coal are from fossil sources and not sustainable. Carbon dioxide emission is the major source for global warming[1] but also released as a byproduct from microbial fermentation processes, for example from biogas in a sustainable waste management. Biogas is a combination of methane (50-75%), CO_2 (25-50%), nitrogen (0-10%), and H_2S (0-3%) depending on the fermentation (organic waste) and the microbial anaerobic digestion process.[2] For some applications, such as vehicle fuel or grid injection, it is necessary to fulfill strictly defined specifications and therefore the natural gas needs to be upgraded.

In the final step, the separation of the mixture of CO_2 and CH_4 must be accomplished. Since CO_2 is the major contaminant of biogas, its removal is the most critical step in terms of regard of economics of the entire process, e.g. for transport applications or satisfying pipeline specifications. Biogas can be upgraded to biomethane by removing CO_2 using different technologies such as cryogenic separation, membrane separation, organic physical scrubbing, chemical scrubbing, pressure swing adsorption, and high pressure water scrubbing.[3] Reversible chemical absorption in amine-based solutions can be considered as the most advanced and promising technique for CO_2 capture from flue gas nowadays.[4-6] Since it accounts for 3–6% of the biomethane production cost, the absorbent material for CO_2/CH_4 gas mixture separation requires a high chemical and energy efficiency for the absorption and solvent recovery processes. The development of new CO_2 absorbing processes requires the design of novel, robust and efficient physical organic absorbers.

Modern computational methods and simulations greatly contribute to solutions of such problems but have mostly focused on quantum chemical methods, for some reviews see [7] and [8]. The first principles simulations of CO_2 binding are able to give reaction energy profiles, elucidate alternative reaction pathways and investigate the influence of chemical functional groups on carbon dioxide

absorption but cannot address liquid state properties, such as viscosity, solubility or possible phase separations.

From a computer-based screening of compounds, a set of new and promising CO_2 absorptive solvents were chosen out of hundreds known and novel compounds. [9] From a large set of molecular compounds, a subset of candidate molecules was evaluated as to their thermodynamic, and kinetic properties taking into account the concept of sustainability by using the group-contribution statistical associating fluid theory for square well potentials (SAFT-γ SW) . We here use a representative subset of four alkanolamine compounds; the well-characterized monoethanolamine (MEA) as a standard and benchmark, and three representatives for each classification of amines: a primary amine 3-aminopropanol (MPA), a secondary amine 2-methylaminoethanol (MMEA) and a tertiary amine 4-diethylamino-2-butanol (DEAB), see Figure 1.

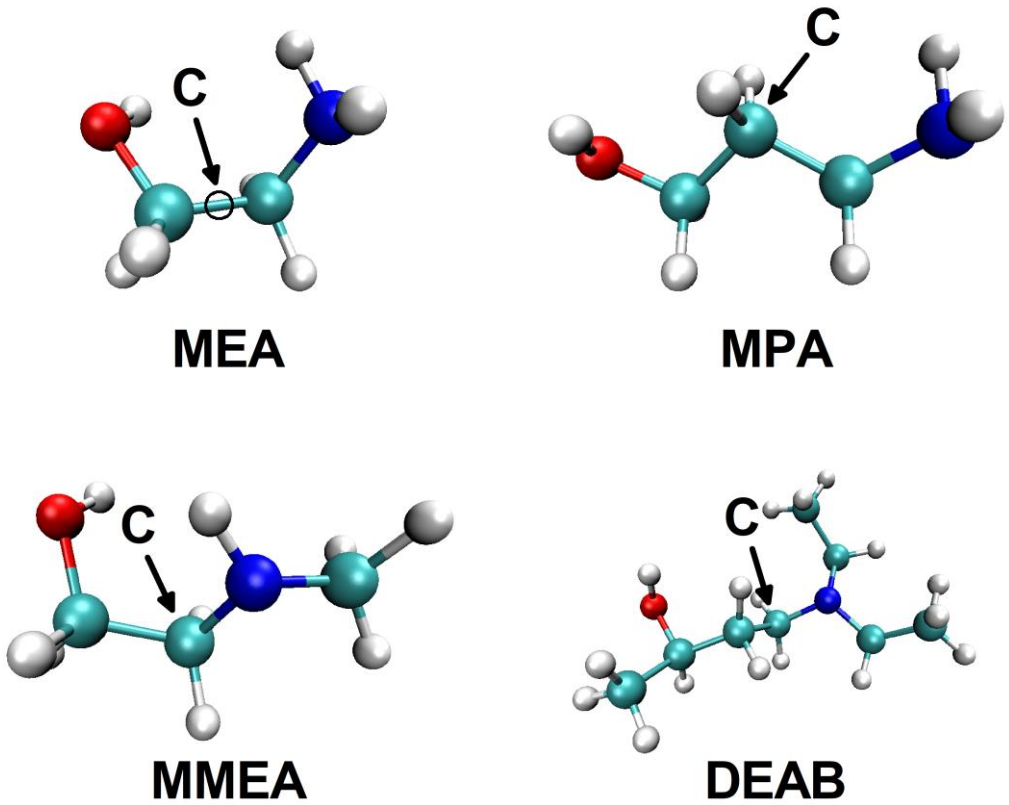

Figure 1. Four high-performance and sustainable alkanolamine compounds for CO_2 sequestration from biogas in their low energy conformation in aqueous solution. MEA (monoethanolamine) was used as a standard and reference compound and compared with another primary amine 3-aminopropanol (MPA), a secondary amine 2-methylaminoethanol (MMEA) and a tertiary amine 4-

diethylamino-2-butanol (DEAB) as to their properties in ternary mixtures with CO_2 and water. The marked spot is used to analyze the liquid structure of complex mixtures by means of the radial density functions (RDFs).

Molecular simulations are able to provide detailed insight into liquid solution behavior and to calculate relevant compound-specific thermodynamic and transport properties, for novel CO_2 absorbing compounds[8], some of which are not available in the literature and not accessible experimentally. For example, the diffusion coefficients of CO_2 in these absorptive alkanolamine solvents are not possible to measure experimentally because of the high reactivity in the amine solution. Very often, one then resorts to the diffusion coefficients of the related N_2O in solution, for a review see.[10] There is, however, recent evidence for the validity of this CO_2/N_2O analogy for dilute solutions only and an apparent lack of VLE data for CO_2 and N_2O. Continuous fractional component Monte Carlo (CFCMC) simulations showed that the CO_2/N_2O analogy was valid for a 30% aqueous MEA solution at 303 K.[11]

In the current paper, we are investigating the structural and dynamic features of CO_2 molecules in aqueous alkanolamine solutions over a wide range in temperature and solvent compositions. Previous molecular simulations of CO2 solvation in alkanolamine solutions were limited to single compounds or a few mixture compositions only. The liquid structure of CO_2-MEA and CO_2-water interactions for a particular composition were reported in [12,13]. The diffusion coefficients of CO_2 solvated in MEA/W mixtures[11,14] and in mixed alkanolamine solutions were also calculated.[15] The statistics of collision between amine nitrogen atoms and CO_2 in aqueous was simulated in reference [16] and the spatial distribution of CO_2 around two examples of alkanolamines are given in [17]. The properties of CO_2 in mixed solution of four tertiary alkanolamines were investigated in reference[18]. Most of the previous studies were addressing fundamental issues of aqueous MEA as an absorptive solvent. They provide only individual insight into the molecular structure of ternary (CO_2/alkanolamine/water) mixtures and transport properties of CO_2.

In this paper, we present the first systematic MD study of the solvation and mobility of CO_2 in a representative set of novel compounds and use MEA as a reference and standard. The analysis of CO_2 interactions with alkanolamine molecules as a function of changes in solvent composition (from pure alkanolamine towards water-rich aqueous solutions) and temperature (relevant temperature range for practical application of 298-323 K) give a complete picture of the solvation, dynamics and kinetics of CO_2 in alkanolamine/water mixtures for a range of compounds of different chemical classes. The results for MPA, MMEA and DEAB in comparison to MEA allow a detailed assessment of their individual properties and features which need to be considered when suggesting new classes of compounds for CO_2 sequestration.

Primary and secondary amines display preferential interactions with solvent water molecules and less so with carbon dioxide. In aqueous solution, CO_2 diffusion is fast and residence times are short. DEAB as a novel alkanolamine carbon dioxide-absorbing compound, however, displays favorable structural and kinetic features for CO_2 sequestration from biogas.

Computational Methods and Details

Alkanolamines, water and carbon dioxide were modelled using the all-atom optimized potentials for liquid simulations (OPLS-AA) forcefield[19], the charge/extended (SPC/E) model for water[20] and the transferable potentials for phase equilibria (TraPPE) force-field for CO_2.[21] This choice of forcefields was shown to give accurate results for alkanolamines and water solutions over a wide range of temperature and concentration.[22] The reliability of the TraPPE forcefield for modelling CO_2 solubility and diffusivity in water, ethanol and aqueous MEA was validated before.[11] Long-range electrostatic interactions were treated with the particle-mesh Ewald algorithm. Non-bonded interactions were modelled with a 12−6 Lennard-Jones potential. A cutoff radius of 1.4 nm was used for all interactions. Lennard-Jones parameters for unlike interactions were calculated using the geometric average rule.

MD simulations were carried out with Gromacs 5.1.2[23] in a temperature range from 298 to 323 K. The following sequence of simulations was performed for each alkanolamine type and aqueous mixtures. Initially, the corresponding amount of alkanolamine, water and CO_2 molecules were randomly placed in a simulation box, which size was a bit larger than the nominal volumes for pure mixture components, and an energy minimization was carried out. Then, an isothermal−isobaric (NPT) ensemble 2 ns simulation run (preceded by 500 ps of equilibration) was performed to define the solvent density and simulation box size for the next simulation stage. A Berendsen thermostat and barostat[24] with coupling parameters of 0.2 and 2 ps were used to maintain temperature and pressure. Then, a canonical (NVT) ensemble 20 ns simulation run (preceded by a 1 ns equilibration run) was carried out. A Nosé−Hoover thermostat[25,26] with a coupling constant of 0.4 ps was used for temperature control. The equations of motion were integrated with a time step of 1.0 fs in both ensembles. Simulation trajectories were saved every 1 ps for further data analysis. CO_2 molecules were solvated at a concentration of about 0.2 M (0.1 M for DEAB cases) in aqueous alkanolamines which refers to typical experimental loadings. Simulations were carried out for alkanolamine/water solvent ratios of 7.5/92.5 (6/94 for the case of MEA), 30/70, 50/50, 80/20, and 100/0 (pure alkanolamine) (w/w) for the four molecule types. The number of molecules and simulation box size dimensions for all studied molecular ensembles are provided in the Supporting Information. The required simulation box size dimensions were determined from preliminary simulations and checked for an absence of finite size effects.

The spatial distribution function (SDF) provides a 3-dimentional view of the preferential distribution of a molecule (or atom) around a reference molecule. The combination of one dimensional radial distribution functions (RDFs) with SDFs represents a very powerful tool of analysis to characterize and visualize solvent structure at the molecular level. SDFs of CO_2 around alkanolamines were generated with the TRAVIS package.[27] Diffusion coefficients were calculated from the mean square displacement and the observation time (over a 100−500 ps time interval). The residence autocorrelation functions describe the probability of a CO_2 molecule to stay close to an

alkanolamine molecule over time and were calculated as described in[28]. As a criterion for a CO_2 molecule to be close to an alkanolamine molecule, the distance obtained from the $C_{alkanolamine}$-C_{CO2} RDF was used (the radial coordinate of the first minimum).

Results and Discussion

Liquid densities of ternary CO_2/water/alkanolamine solutions and hydration of amines.

At the studied CO_2 concentrations of 0.1-0.2 M, the simulated liquid densities of alkanolamine/water/CO_2 ternary mixtures do not significantly differ from those of the previously simulated two component solvents (alkanolamine/water)[22] and are in good agreement with experiment[29] (see Table 1). This shows that the flow and solvation of CO_2 at common loadings hardly affect the system's bulk properties.

For example, for 30% (w/w) solutions of alkanolamine in water, the solution density only change by 0.2-0.4%: from 1019.7 kg m^{-3} to 1021.9 kg m^{-3} in the presence of CO_2 for MEA and from 979.8 to 973.0 kg m^{-3} for DEAB. At lower concentrations of water, the effect of introduction of carbon dioxide is less pronounced and almost vanishes.

Table 1 Liquid densities (kg m^{-3}) for binary alkanolamine/water and ternary alkanolamine/water/CO_2 mixtures at T=298 K.

Composition %wt of alkanolamines	MEA			MPA			MMEA			DEAB		
	Binary (MEA/water)		Tertiary (MEA/water/CO_2)	Binary (MPA/water)		Ternary (MPA/water/CO_2)	Binary (MMEA/water)		Ternary (MMEA/water/CO_2)	Binary (DEAB/water)		Ternary (DEAB/water/CO_2)
	exp[a-c]	*sim*	*sim*	*exp*[d]	*sim*	*sim*	*exp*[e,f]	*sim*	*sim*	*exp*[g]	*sim*	*sim*
100	1011.7	1036.0	1037.4	997.2	1011.3	1014.2	937.7	926.7	927.6	860.0	877.1	877.0
80	1024.7	1042.4	1043.8	1005.9	1024.3	1025.2	-	968.5	968.5	-	915.2	915.7
50	1021.3	1032.0	1033.5	1008.2	1022.6	1024.2	1000.2	996.9	997.7	-	956.1	953.2
30	1010.0	1019.7	1021.9	1003.7	1013.2	1015.4	999.2	1000.9	1002.6	982.0	979.8	973.0

7.5	999.1*	1000.3*	1005.4*	-	1002.7	1004.7	996.4	999.4	1002.0	-	996.8	997.8

[a]Data from ref [30]. [b]Data from ref [31]. [c]Data from ref [32]. [d]Data from ref [33]. [e]Data from ref [34]. [f]Data from ref [35]. [g]Data from ref [36].

* For the MEA case this composition is the 6/94 w/w MEA/W.

In general, the solution densities of the ternary mixtures increase by a less than 0.2% compared to that of the binary alkanolamine/water solutions. This is in agreement with previous results where a change of only a few percent of volume per amine molecule was observed even for high loadings of carbon dioxide.[37]

Addition of carbon dioxide does neither affect the dominant molecular conformation of the alkanolamine molecules in solution. Also the alkanolamine and alkanolamine-water RDFs are not perturbed in the presence of CO_2 molecules and virtually identical to those of the binary solutions[22] and are not shown here. That is why we focus on characterizing the intermolecular interactions of carbon dioxide with alkanolamine and water molecules.

Structural classification of ternary CO_2/water/alkanolamine solutions.

Radial Distribution Functions (RDFs) are one-dimensional representations of an interatomic or intermolecular distance averaged over entire MD trajectories, e.g. they describe how close the two particles of interest approach each other. The RDF function $g(ij, r)$ describes the relative probability of finding a pair of atoms i and j at the distance r apart and relative to that of a uniform distribution at the same density.[38]

Figure 2 shows the RDFs of CO_2 and solvent water (dotted and dashed lines) and the four alkanolamine molecules (solid lines) for a representative composition of 30/70 (w/w) of alkanolamine/water at T=313 K.

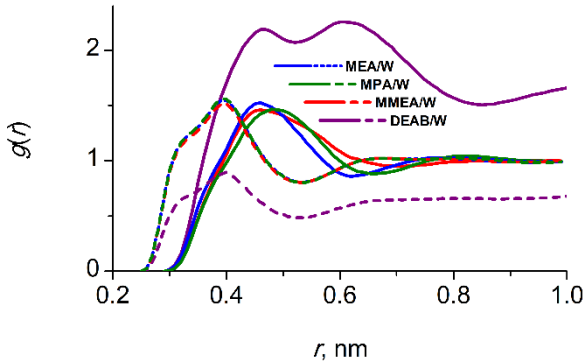

Figure 2 Liquid structures of ternary mixtures of CO_2/water/alkanolamine. RDFs of C_{CO2}-$C_{alkanolamines}$ (solid curves) and C_{CO2}-O_W (dotted and dashed curves) for the 30/70 (w/w) solution composition of alkanolamine/water at T = 313K. Blue, green, red and purples colors designate MEA, MPA, MMEA and DEAB compounds.

For aqueous MEA, MPA and MMEA solutions, the peaks of the RDFs for CO_2-water interactions (dotted and dashed lines) and CO_2-alkanolamines (solid lines) are almost indistinguishable between the compounds (see Figure 2). This indicates that the water-CO_2 and alkanolamine-CO_2 interactions are almost identical for these primary and secondary amines MEA, MPA and MMEA. The equal peak amplitudes for interactions with water (at r = 0.40 nm) and alkanolamines (at r = 0.49 nm) show that the CO_2 molecules are evenly distributed between the alkanolamine and water solvents and there is no preference of solvation with either of them. Also in the absence of CO_2, the binary solutions of the primary amines MEA, MPA and the secondary amine MMEA display identical RDFs for the interaction with water.[22] We conclude that this set of compounds displays very similar solvation and solvent interactions with water and CO_2 molecules.

DEAB as a tertiary amine behaves differently. In water, the DEAB molecules tend to self-associate and start to form large hydrophobic clusters which here accommodate CO_2 molecules. The RDF peak amplitude for the carbon dioxide-DEAB interaction is significantly more pronounced than that for CO_2-water (see Figure 2). This demonstrates a clear preference of CO_2 to reside in close vicinity of the DEAB molecules and clusters and avoid hydration (see below).

In the following, we are going to analyze in more detail the RDF for MPA at various concentrations. Since molecule hydrophilic interactions of the hydroxyl and amine groups with the solvents are separated by three methyl groups in that molecule, the discrimination between hydrophilic and hydrophobic interactions is more distinct. The discussion, in analogy, also holds for the RDFs for MEA and MMEA which are given in the Supporting Information.

Localization of CO_2 molecules in aqueous MPA solutions.

Since aqueous MEA, MMEA and MPA solutions display very similar structural features in the presence of CO_2 (see above), only the results for MPA will be discussed here in detail. The approach and association of solvated CO_2 molecules in aqueous MPA is characterized with the help of RDFs (Figure 3), spatial distribution functions (SDFs) of CO_2 and water around an MPA molecule (Figure 4) and visualized by simulation snapshots (Figure 5).

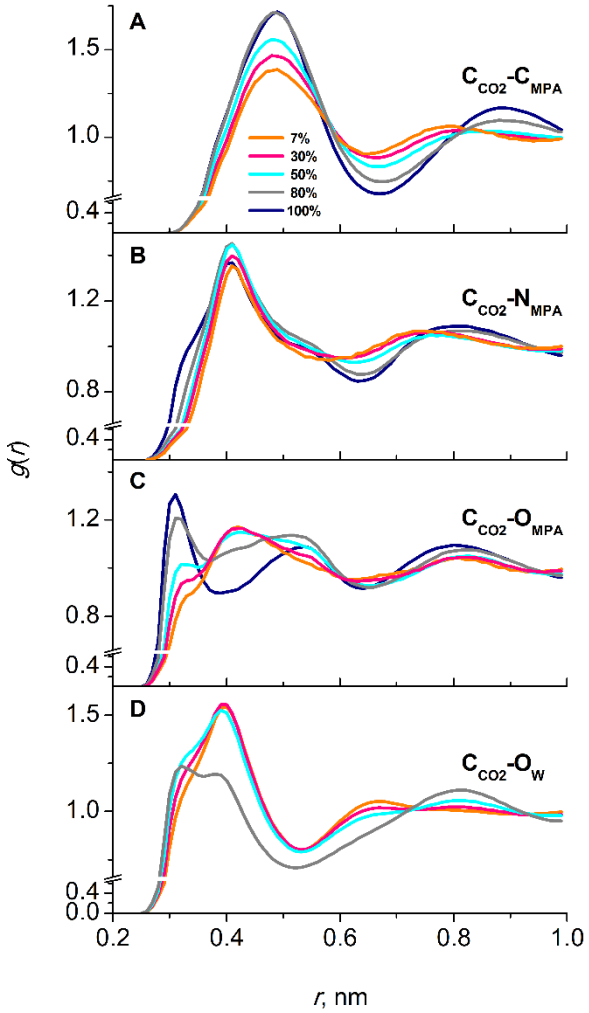

Figure 3 Further liquid structure details of the ternary mixture of CO_2/water/alkanolamine. Results are shown here for MPA (for MEA and MMEA they can be found in the Supporting Information). Selected RDFs between carbon dioxide and MPA and water at ratios of MPA/water (w/w) of 7.5/92.5 (orange curve), 30/70 (pink), 50/50 (cyan), 80/20 (gray), and 100/0 (navy).

In aqueous MPA, the carbon dioxide molecules display no clear preference for interacting with either the alkanolamine compound or water. This information is obtained from the fact that the first peaks of the RFDs of CO_2 interactions with MPA (Figure 3A) and water (Figure 3D) are of approximately equal amplitude, except for the 80/20 (w/w) MPA/water system (which we discuss in detail below). This effect was also reported for aqueous MEA solutions.[12]

The broad peak at about r = 0.49 nm in the C_{MPA}-C_{CO2} RDF curves (see Figure 3A) originates from CO_2 molecules of the first solvation shell of MPA. One can discriminate between CO_2 alkanolamine interactions which are hydrophobic in nature with the carbon chain atoms (Figure 3A) and polar with the amine nitrogen (Figure 3B) and the hydroxyl groups (Figure 3C).

The polar CO_2-MPA interactions (Figures 3B and 3C) decrease in RDF peak amplitude upon increase of water content since the carbon dioxide molecules interacting with MPA are being displaced by water molecules which form strong hydrogen bonds with the amine and hydroxyl groups of MPA. The exchange of CO_2 by water thus leads to a decrease of the effective first solvation shell radius, which can be seen in the shift of the second peaks in the RDF from r = 0.86 nm (at 100%, 80% and 50% MPA) to r = 0.79 nm (at 30% and 7% MPA, see Figure 3A).

The major five CO_2 orientations with respect to MPA are displayed in Figure 4. Since the radial distribution function (RDF) is an orientation average over the angular coordinates, detail information of the local solution structure is lost. The spatial distribution function (SDF)[39] incorporates the radial and angular coordinates of the interatomic interactions and describes the three-dimensional density distribution of intermolecular interactions in a local coordinate system.

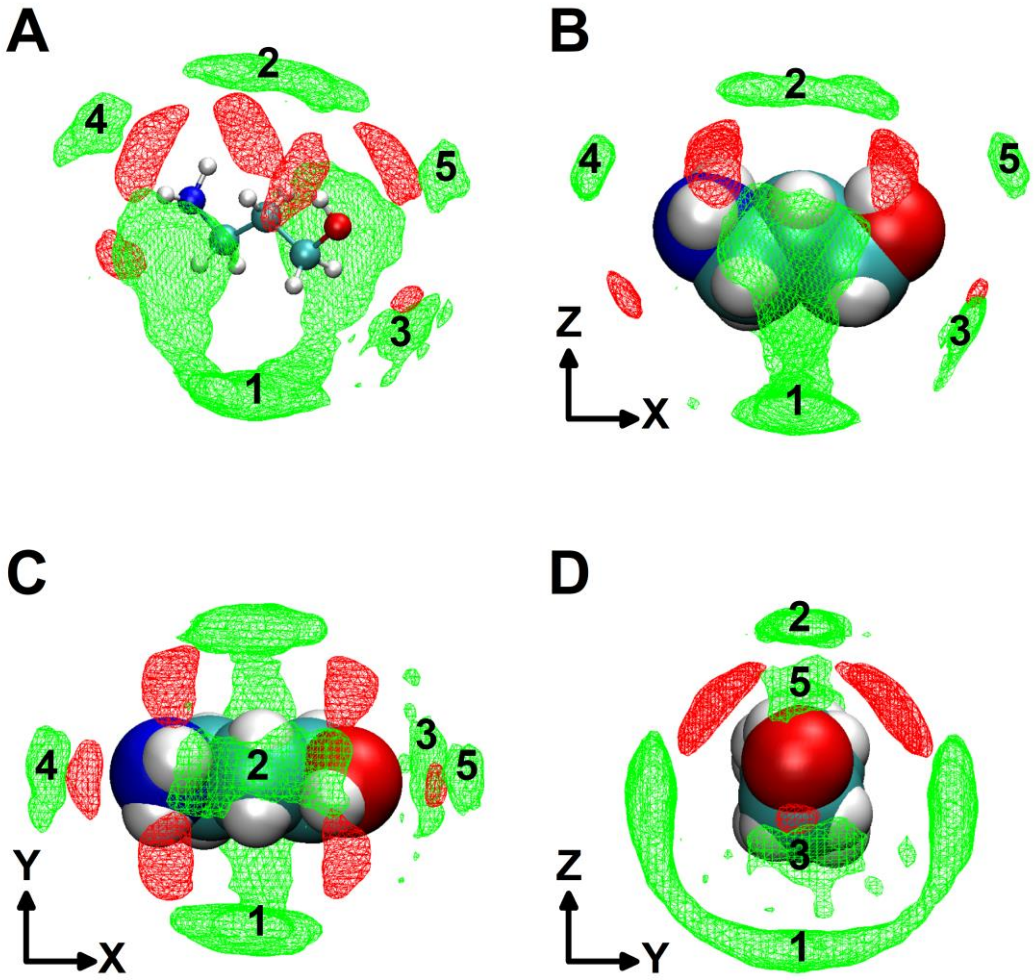

Figure 4. Preferential localization of CO_2 (green) and water (red) molecules in vicinity of MPA. 2D projections of the spatial distribution functions (SDFs) of carbon atoms of carbon dioxide (green color) and oxygen atoms of water (red color) around MPA molecule at a 30/70 (w/w) MPA/water composition. Iso-surfaces are drawn at a density level of 50%. The five main localizations of carbon dioxide around MPA molecule are numbered (see text for a discussion). Water molecules are located mainly in three distinct regions around the rotating the amine and hydroxyl groups of MPA with which they can form hydrogen bonds and act either as an acceptor or a donor.

Region 1 in Figure 4 is the dominant location of CO_2 in the vicinity of MPA. It refers to the hydrophobic interaction of CO_2 with the carbon chain methyl groups of MPA in an orientation quasi-parallel to the MPA molecular axis (see Figure 5A).

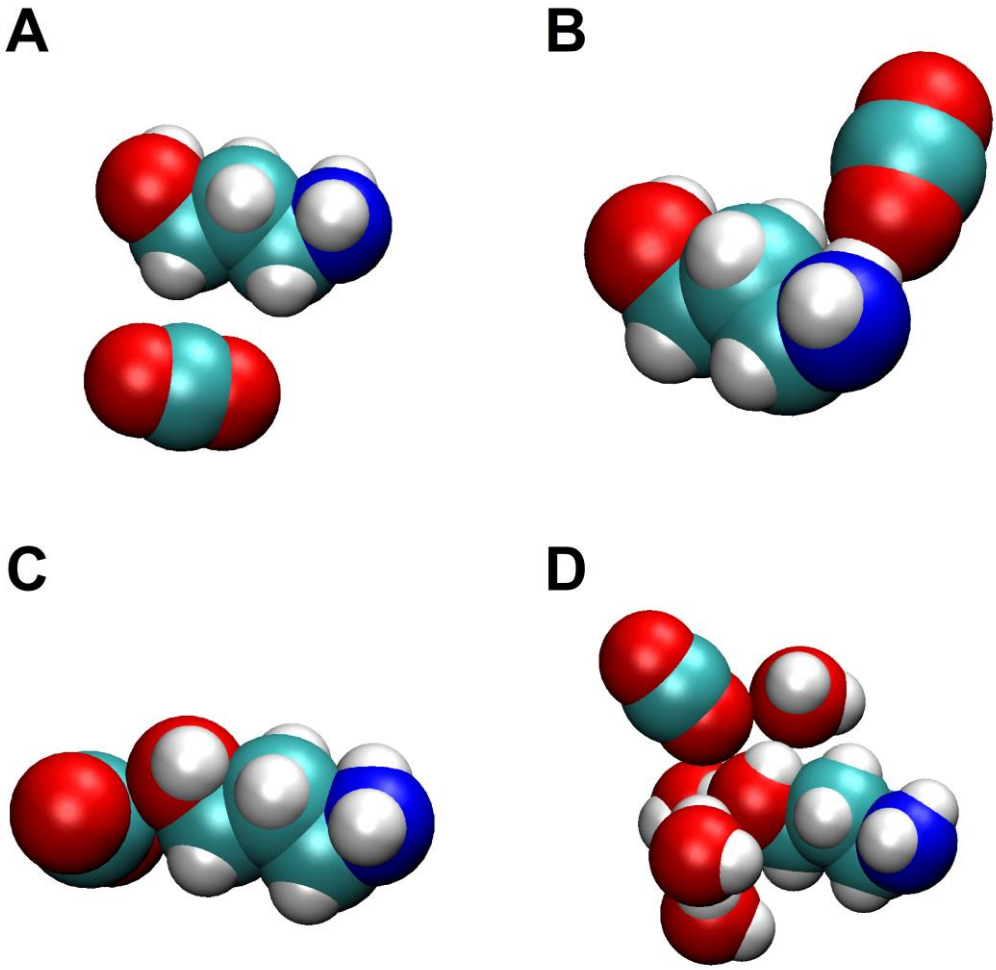

Figure 5 Characteristic snapshots from MD simulations showing the most relevant orientations of the first solvation shell of carbon dioxide molecules in the vicinity of the MPA molecule.

As to the polar interactions between CO_2 and MPA, three types can be distinguished from Figures 3B and C and Figure 4.

- A direct interactions of the N_{MPA} and C_{CO2} atoms occurs only very rarely and can only be seen as a small shoulder in the RDF (Figure 3B) at r = 0.32 nm. The SDF regions 2 and 4 in Figure 4 are instances in which the O atoms of carbon dioxide act as hydrogen bond acceptors of the NH_2 group protons (see Figure 5B). This corresponds to the large peak at r = 0.41 nm in Figure 3B.
- One of most frequent CO_2-MPA orientations is shown in Figure 5C. The shoulder of the RDF at r = 0.55 nm (Figure 3C) corresponds to CO_2 molecules acting as hydrogen bond

acceptors of the hydroxyl group protons of MPA. The same information is also be obtained from an analysis of the HO_{MPA}-C_{CO2} RDFs.

Upon increase of the water content, the water molecules displace CO_2 molecules from positions close to the oxygen O_{MPA} and nitrogen N_{MPA} atoms, and the respective peaks in the RDF decrease in amplitude and the interaction radius between O_{MPA} (N_{MPA}) and C_{CO2} atoms increases to r = 0.41 nm (Figure 3C). Such a relative molecular orientation can be seen in Figure 5D. More SDFs which show the preferred localization of CO_2 and water molecules around MPA at various mixture compositions are presented in the Supporting Information.

The hydration of carbon dioxide (Figure 3D) shows an intermolecular distance of r = 0.40 nm between the C_{CO2}-O_w atoms for the first solvation shell. At 80/20 (w/w) MPA/water composition, the amplitude for that radial coordinate significantly decreases and also the first minimum of the RDF (at r = 0.33 nm) becomes smaller and broader. At this mixture composition, the MPA/water phase separation sets in and the water molecules are forming small isolated clusters which was also observed for binary mixtures of water and MEA.[22] Carbon dioxide is excluded from these clusters but interacts with a few isolated water molecules in the vicinity of the polar groups of MPA.

The same line of argumentation also holds for ternary mixtures water of CO_2 and the MEA and MMEA alkanolamine compounds and is not repeated here (see the Supporting Information).

Localization of CO_2 molecules in aqueous DEAB solution.

The behavior of carbon dioxide in aqueous solutions of DEAB is significantly different from that in MEA, MMEA and MPA. Figures 6, 7 and 8 give structural information about the intermolecular distances, preferential localization of approaching CO_2 and relative orientations of carbon dioxide in aqueous solution of DEAB.

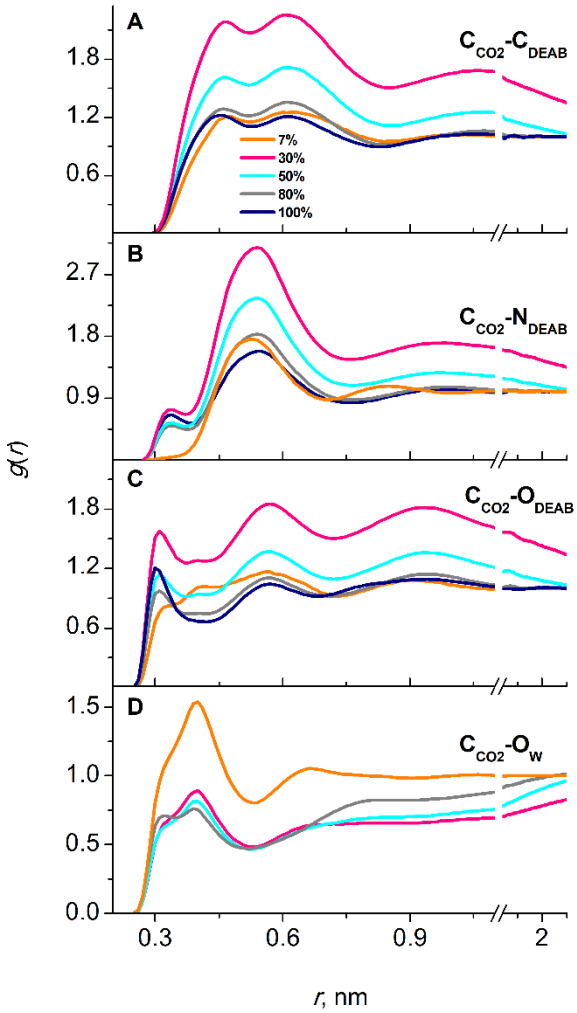

Figure 6 Complex liquid structure of ternary mixtures of CO_2/water/DEAB at different solvent compositions. The RDFs of intermolecular interactions of carbon dioxide, DEAB and water at ratios of DEAB/water (w/w) of 7.5/92.5 (orange curve), 30/70 (pink), 50/50 (cyan), 80/20 (gray), and 100/0 (navy).

Whereas the interactions of CO_2 with primary and secondary amines were equally distributed between water and the absorbent, the RDFs of CO_2 molecules in aqueous DEAB at various DEAB concentrations (Figure 6 A-C) show that the carbon dioxide molecules are preferentially located in close vicinity to DEAB molecules and avoid water. The amplitude of the RDF for CO_2–water interactions (Figure 6D) is lower than for the CO_2-DEAB interactions with C_{DEAB}, N_{DEAB} and O_{DEAB} (Figure 6 A-C). Second, the RDF peak amplitudes for CO_2-water interactions are less than 1 for DEAB concentrations above 7%. This indicates that the probability of CO_2-water interactions is less likely than expected from the nominal composition. At increasing water concentration, this

preference becomes more pronounced which can be seen in the increase of all the CO_2-DEAB peak amplitudes (Figure 6A-C). The CO_2-DEAB RDF peaks increase in amplitude until a 30/70 (w/w) DEAB/water composition, and then decrease at higher water content. This effect is also seen for the intermolecular DEAB-DEAB interactions and shows that the distribution of CO_2 molecules around DEAB molecules is independent of the amount of water in solution, except for the dilute 7.5/92.5 (w/w) DEAB/water mixture.[22]

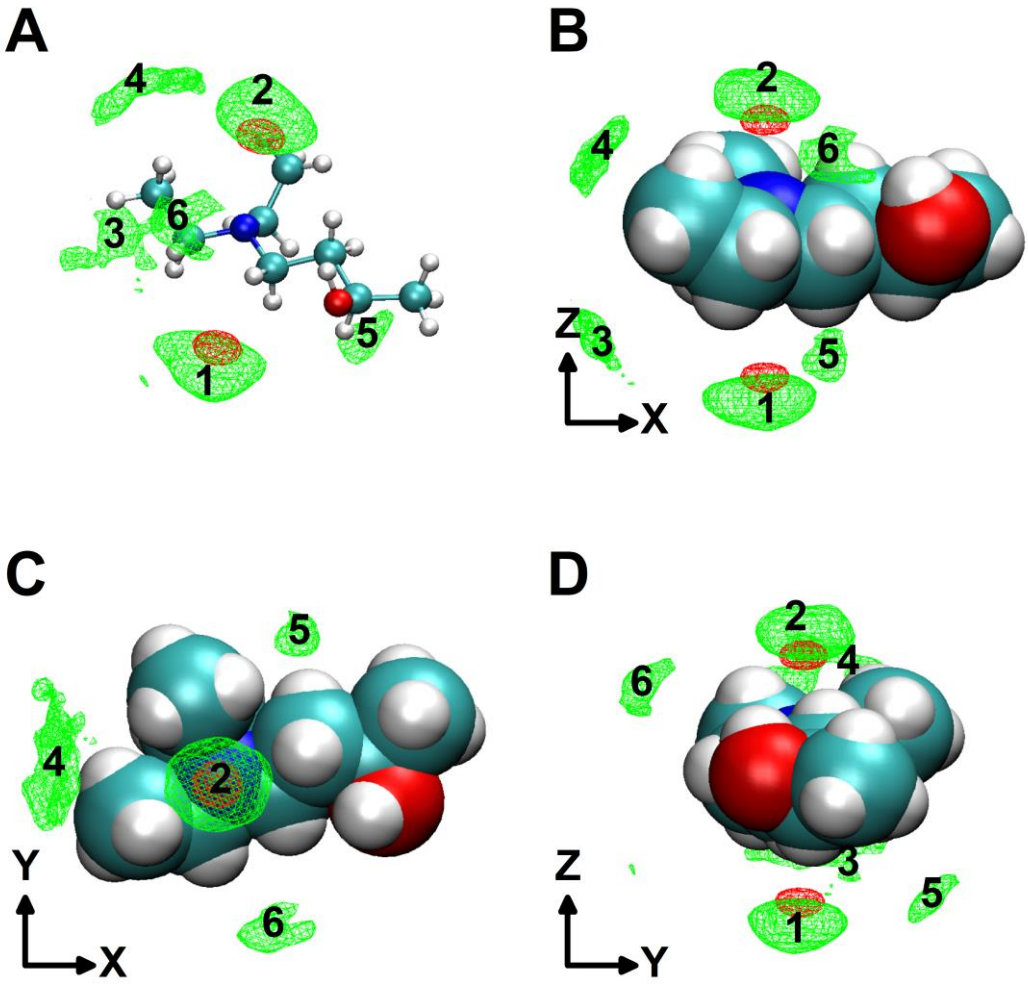

Figure 7 Structural mapping of the preferential localization of first solvation shell carbon dioxide (green) and water (red) molecules with respect to DEAB. The spatial distribution functions (SDFs) of carbon atoms of CO_2 and oxygen atoms of water around a DEAB molecule are shown at the 30/70 (w/w) DEAB/water composition. The main chain carbon atoms are used to define the coordinate system. Iso-surfaces are drawn at 50%. The dominant five locations of carbon dioxide

around the DEAB molecule are numbered (see text). Water molecule positions are shown for only two major sites of interaction close to the amine nitrogen of DEAB to which they form hydrogen bonds. Water interaction with the hydroxyl group are less prominent cannot structurally be mapped.

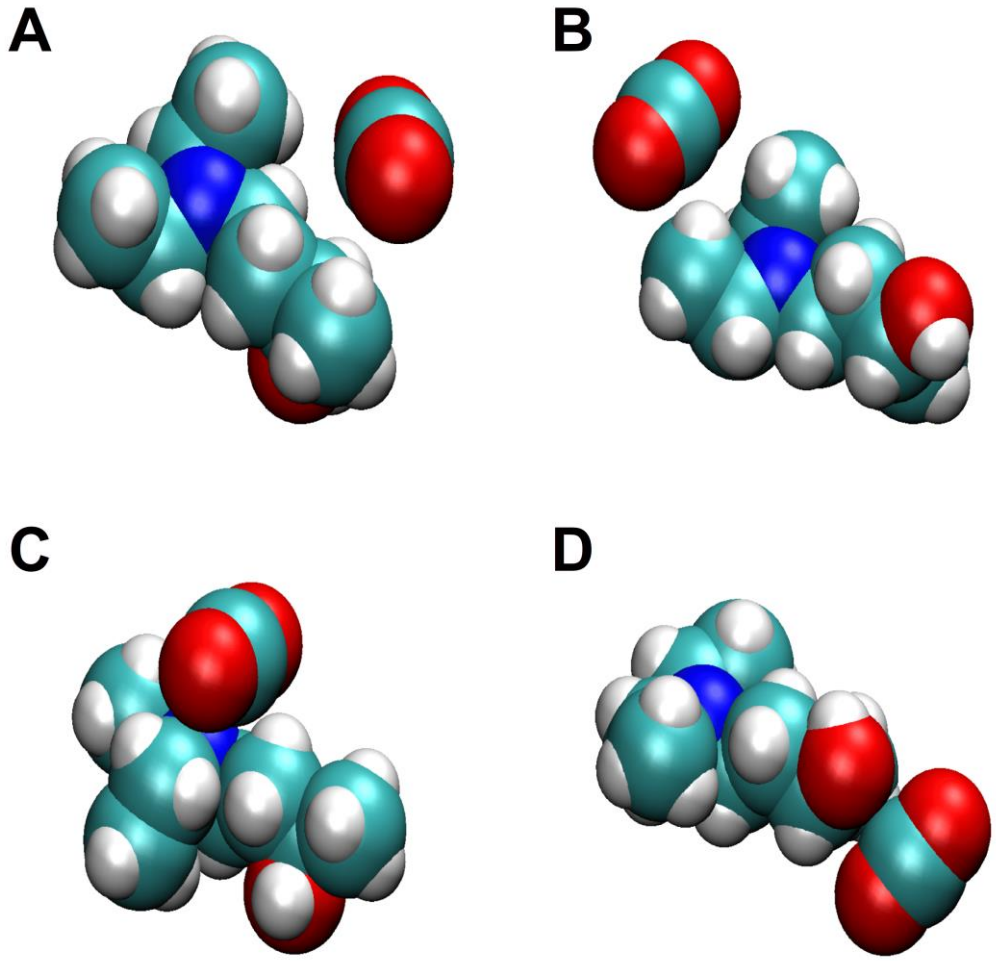

Figure 8 Representative snapshots from MD simulations showing the dominant association channels of carbon dioxide approaching DEAB molecule.

On average, each nitrogen atom of DEAB molecule forms about 0.97 hydrogen bonds with water at a composition of 7.5/92.5 DEAB/W (w/w) and 0.47 hydrogen bonds at 80/20 DEAB/W (w/w).[22]

From the SDFs (Figure 7), we can identify several sites of interaction between CO_2 and the alkanolamine DEAB.

- First, the peak position at a distance of 0.47 nm in the C_{DEAB}-C_{CO2} RDF (Figure 7A) reflects the hydrophobic interactions with alkyl moiety of DEAB (see locations 5 and 6 in Figure 7 and the representative snapshot in Figure 8A). The CO_2 molecules tend to arrange perpendicular to the alkyl chain due to steric interactions with the diethylamine group (see the Supporting Information).
- The second peak at r = 0.62 nm (Figure 7A) refers to CO_2 molecules interacting with the diethyl groups of DEAB (regions 3 and 4 in Figure 7 and the snapshot in Figure 8B).
- The second CO_2 solvation shell at a distance of r = 1.1 nm (Figure 7A) is almost independent of a change in solution composition, unlike in the MPA case. This suggests that CO_2 molecules remain close to the DEAB molecule clusters even at a high content of water and the intermolecular distances do not change.
- The N_{DEAB}-C_{CO2} RDF (Figure 7B) reveals a first small peak at r = 0.33 nm which originates from CO_2 molecules closely approaching the N_{DEAB} atom (regions 1 and 2 in Figure 7, and the snapshot in Figure 8C). These CO_2 approaches occur along spatially well-define and confined regions of and that is why they appear clearly distinguishable in Figure 7. Only at the water rich 7.5/92.5 solution composition, this peak vanishes since water molecules displace the CO_2 molecules from interacting with the N atom and form a strong hydrogen bond network with other water molecules in the surrounding of DEAB (here the DEAB fraction is only 1% molar).
- The large broad peak at r = 0.55 nm (Figure 7B) stems from CO_2 molecules interacting with the hydrophobic chains of DEAB and corresponds to regions 3-6 in Figure 7 (for a discussion see above). The peaks at r = 1.0 nm correspond to the second solvation shell of DEAB by CO_2 and are independent of the solvent composition (see above).

- A direct interaction between CO_2 and the alkanolamine DEAB is to be seen from the first peak at a distance of r = 0.31 nm of the C_{CO2}-O_{DEAB} RDF (Figure 7C) and the representative

snapshot in Figure 8D. Only in the dilute 7.5/92.5 (w/w) DEAB/water mixture, CO_2 molecules are solvated by the water molecules which form hydrogen bonds with the OH group of DEAB.

The RDFs for water-CO_2 (Figure 7D) corroborate the result of the preference of CO_2 to remain in close proximity to the DEAB clusters and avoid hydration by water molecules. The amplitudes of the first peak are below than 1 for all compositions, except for the dilute 7.5/92.5 (w/w) DEAB/water system. The decrease in amplitude at a distance of r = 1 nm with increasing water concentration (for 80/20, 50/50 and 30/70 (w/w) DEAB/water compositions), is a clear evidence of the self-clustering of DEAB molecules and a capture CO_2 molecules in those hydrophobic clusters.

The dynamics of CO_2 in aqueous alkanolamine solutions.

Diffusion coefficients are macroscopic characteristics of the microscopic molecular mobility in solution. Molecular diffusion coefficients are very important parameters in the engineering, simulation and optimization of chemical processes. The diffusion coefficients of CO_2 in different alkanolamine/water solutions, however, are experimentally not accessible due to the spontaneous chemical reactivity of the molecule with the amine. That is why all published CO_2 diffusion data in alkanolamines are only estimates and derived from N_2O mobility analysis. There is recent evidence that the use of the ratio of the solubility of N_2O to that of CO_2 in water may be restricted to dilute systems only. The use of the CO_2/N_2O data extraction requires reliable experimental Henry constants of CO_2 and N_2O in water. There is a remarkable lack of VLE data on the N_2O–water system in literature which prompted the computation of CO_2 diffusion coefficients in complex mixtures.

CO_2 diffusion coefficients in aqueous alkanolamine solution can be obtained from the velocity autocorrelation function in MD simulations. In Figure 9, the simulated CO_2 diffusion coefficients in MEA and DEAB solvents are compared with experiment estimates from N_2O diffusion

measurements.[40-43] The computed diffusion coefficients are in excellent agreement with available experimental N_2O diffusion data rescaled to CO_2 between 298 and 323 K and 30% and 50% enriched alkanolamine solutions, which shows the accuracy of our computational approach. Apparently, for these mixture compositions the use of rescaled N_2O diffusion coefficients seems appropriate. The results for all alkanolamine molecules are given in the Supporting Information.

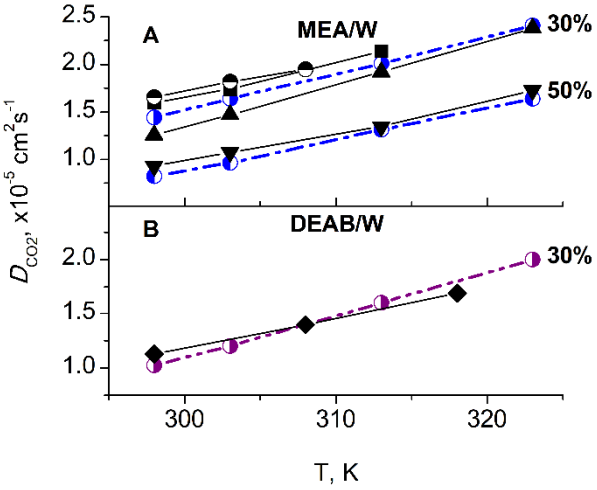

Figure 9 Comparison of experimental and simulated diffusion coefficients of carbon dioxide in aqueous alkanolamine solutions. Black symbols are experimental data from various sources and were derived from nitrous oxide diffusion[40-43]. The colored symbols (semi-filled blue and purple) are computed diffusion coefficients for aqueous MEA and DEAB solutions. The weight fraction composition of alkanolamine solutions in water is given.

Figure 10 shows the CO_2 diffusion coefficients for all investigated CO_2-absorbing alkanolamine compounds in solutions over a wide range from 7.5 to 100% weight percent and in a temperature range from 298 to 323 K. As expected, the diffusion coefficient increases with temperature for all aqueous alkanolamine solutions. For water-rich compositions, the diffusion of CO_2 increases in the following order MEA > MPA = MMEA > DEAB. For dilute solutions between 7.5 and 30%, the CO_2 diffusion coefficient increases linearly with temperature. As the alkanolamine fraction increases, the carbon dioxide diffusion becomes slower due to steric hindrance and an increase in solvent density. The higher the alkanolamine concentration the slower CO_2 diffuses in solution. Above a weight fraction of 50%, the temperature-dependence of the diffusion coefficient deviates

from linearity and the system deviates from ideal behaviour.[10] The same effect is also observed for the diffusion the alkanolamine molecules in water[22].

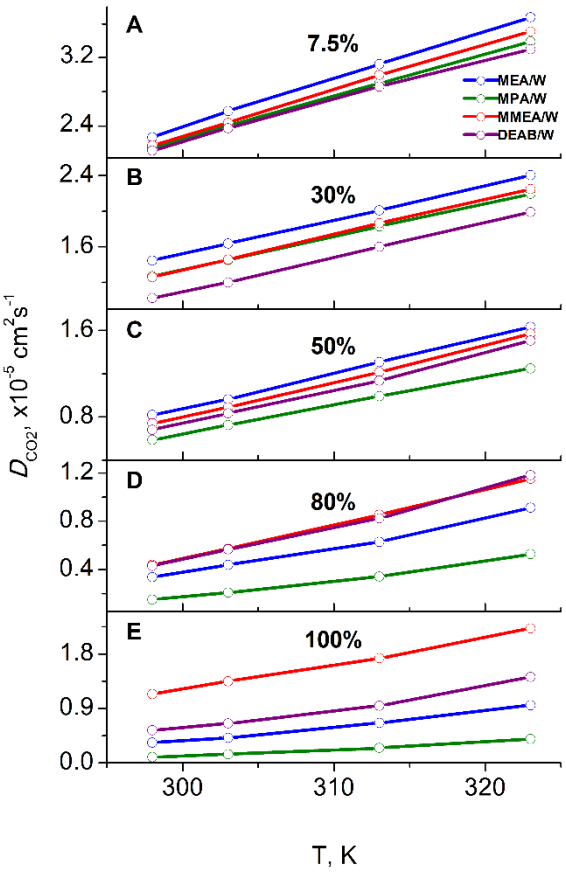

Figure 10 Temperature dependence of carbon dioxide diffusion coefficients in aqueous alkanolamine solutions at various mixture compositions: MEA (blue color), MPA (green), MMEA (red), and DEAB (purple). The numerical values can be found in the Supporting Information.

A comparison of CO_2 diffusion in the different alkanolamine solutions at a specific temperature of 313 K is given in Figure 11. For low alkanolamine concentrations, the CO_2 diffusion correlates with the molecular size: it is fastest in MEA, MPA and MMEA and slightly slower in DEAB. The ordering of CO_2 diffusion in different alkanolamine solutions, however, changes in alkanolamine-rich solution. For pure MMEA solutions (at 100% weight fraction), the liquid density noticeably decreases by 15% compared to aqueous solutions and the molecule's ability to form hydrogen bonds is about 30% less than for the MEA and MPA molecules. Thus, the CO_2 diffusion in pure MMEA solution becomes faster and exhibits the largest diffusion coefficient.[22]

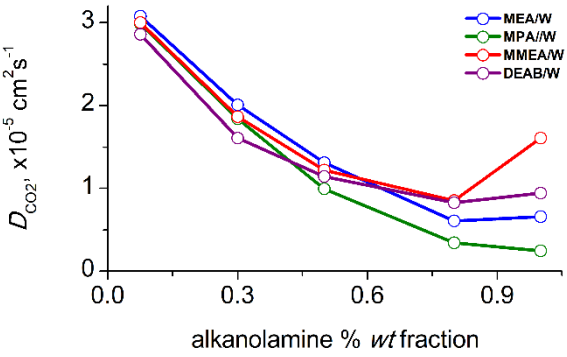

Figure 11 Simulated diffusion coefficients of carbon dioxide in aqueous alkanolamines over the complete range of mixture compositions at a given temperature of T= 313 K.

A similar effect is also observed for DEAB. At concentrations above 80/20 w/w, CO_2 diffuses faster than in MEA and MPA solutions at identical compositions. This enhanced CO_2 diffusion can be attributed to the above discussed preferred localization of CO_2 in hydrophobic DEAB clusters and the avoidance of polar interactions with water molecules. For these amine-rich compositions, CO_2 is to be found in the hydrophobic environment of self-associated large tertiary amines in which it diffuses fast.

Kinetic Aspects of CO_2 Interaction with Alkanolamines in Solution

The average residence time of CO_2 molecules to stay in close vicinity to all alkanolamine molecules in solution was calculated. This information is relevant for the design of novel CO_2 absorbing compounds, since it describes the kinetics of CO_2-alkanolamine interactions in solution. The radius of the first solvation shell from the RDF for each compound was taken as a distance criterion.

The residence autocorrelation functions (see Supporting Information) of the four studied molecules reveal two kinetic components (see Figure 12 and Table 2). The slow component is associated with a residence time in the range of 5-20 ps and the fast one with a residence time in the

range of 0.5-1 ps. The slow component corresponds to direct hydrophobic interactions of CO_2 with the alkanolamine molecules (the alky -CH_2- chain) and the short residence time is related to interactions between the nitrogen atoms of the alkanolamine and the carbon atoms of CO_2. Besides taking into account favorable thermodynamics of CO_2 absorption, the development of novel compounds must also consider the time of interaction of CO_2 and the alkanolamine molecule in solution for the reaction to occur.

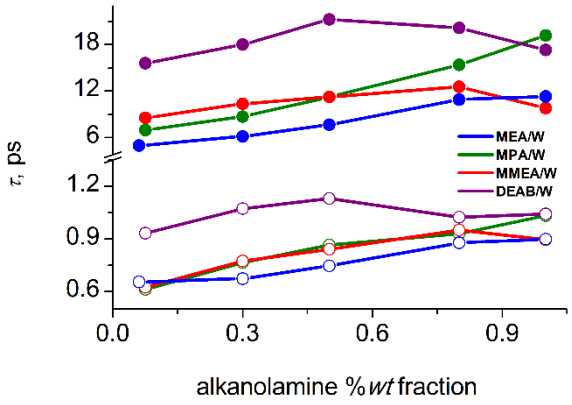

Figure 12 Residence times of CO_2 molecules located next to alkanolamine molecules at T= 313 K. A two-component kinetics of interactions can be seen (see text for details).

These residence times generally follow the same trend as the diffusion coefficients in Figure 10.

Table 2 Calculated two-component residence times (slow (hydrophobic) and fast (polar) components, in ps) of CO_2 molecule located next to alkanolamine molecules in aqueous solution at T= 313 K. For MEA this composition is at 6/94 w/w MEA/W (marked by an asterisk, *).

Composition %wt of alkanolamines	MEA		MPA		MMEA		DEAB	
	fast	slow	fast	slow	fast	slow	fast	slow
100	0.90	11.30	1.03	19.23	0.90	9.81	1.04	17.33
80	0.88	10.95	0.93	15.39	0.95	12.56	1.03	20.15
50	0.75	7.63	0.87	11.24	0.84	11.27	1.13	21.25
30	0.68	6.17	0.76	8.73	0.78	10.36	1.07	18.00

7.5	0.66*	4.94*	0.61	7.00	0.63	8.53	0.93	15.63

At low alkanolamine concentrations, he shortest residence times of CO_2 can be seen for the MEA molecule (with 0.7 ps for the polar and 5-6 ps for the van der Waals interactions, see Table 2) which also displays the fastest CO_2 diffusion. The longest times of residence (0.9-1.0 and 16-18 ps) and the slowest CO_2 diffusion is observed for DEAB. For MEA and MPA adjoining the N atom as the alkanolamine concentration increases, the average residence times become longer since the CO_2 diffusion slows down.

For MMEA and DEAB alkanolamine molecules there is a more complicated relationship between concentration and CO2 diffusion to be seen. For pure MMEA, the residence time decreases relative to a 80% solution because of the above mentioned decrease of the MMEA liquid density and thus the lower ability of MMEA molecules in solution to form hydrogen bonds with the carbon dioxide molecules. For DEAB, this phenomenon already sets in at lower concentrations: the residence times decrease from above a 50/50 composition. The CO_2 molecules then reside in DEAB clusters and move faster in that hydrophobic environment. With an increase of DEAB concentration, the water-free hydrophobic regions become larger and lead to shorter residence times.

Conclusions

Chemical absorptive removal of CO_2 from biogas to fulfil pipeline specifications requires novel and more efficient CO_2-aborbing molecules. Besides thermodynamic properties such as low heat of absorption and ease of solvent recovery, a more comprehensive set of parameters must also be considered related to liquid structure properties such as solubility, diffusion, non-ideality and kinetic aspects. Computer-aided molecular design can provide some of these data which are difficult to obtain or inaccessible by experiment. The absence of certain parameters for alkanolamines in solution is due to experimental difficulties at high amine loadings and the lack of an accurate proper vapor-liquid equilibrium (VLE) model.

Solvent structural details of CO_2 dissolved in aqueous alkanolamine solution of scrubbing compounds with different properties (MEA, MPA, MMEA and DEAB) were obtained over a large range of ternary mixture compositions and a temperature range between 298 – 323 K. Solvent densities, CO_2 diffusion properties and the molecular structure of the complex ternary mixtures can be obtained from molecular simulations but are not available from experiment. The liquid solution densities and the liquid state structure of these ternary mixtures, the most important CO_2-alkanolamine interactions in solutions and the diffusion coefficient of CO_2 molecules could be obtained and reveal a complex system behavior.

CO_2 absorption is a balance between aqueous solvation and desolvation, hydrogen bonding and hydrophobic interactions and very sensitive to the exact composition of the solution. In aqueous solutions of MEA, MMEA and MPA, the solvation and distribution of carbon dioxide is very similar among those molecule and the solute shows no preferential interaction with either water or the alkanolamine. At a water-rich composition of 80/20 w/w alkanolamine/water, water tends to form separate clusters void of CO_2. At increasing of water concentration, the water molecules are forming hydrogen bonding interactions with the hydroxyl and amine groups of the alkanolamines and are displacing CO_2. This shows that at low alkanolamine concentrations CO_2 diffusion and approach is fast and easy for primary and secondary amines but at higher amine loadings hydrophilic interactions with solvent water are obstructing the direct reaction with CO_2.

In aqueous DEAB solutions, however, the solute CO_2 molecules are preferably located inside large clusters of self-associated DEAB molecules with a long residence time. Already at 7.5/92.5 w/w DEAB/water ratio, two DEAB molecules associate and are connected by a water-mediated hydrogen bond network. As a tertiary amine, it does not directly react with carbon dioxide but rather acts as a base which then catalyzes the hydration of CO_2.[44] DEAB (4-diethylamino-2-butanol) was specifically designed as a molecule with high CO_2 binding affinity [45] and predicted to have a lower degree of toxicity than MEA.

The development of novel CO_2 sequestrating compounds is asking for a thorough investigation not only of their thermodynamic ability to absorb carbon dioxide but also their kinetic and liquid phase properties. Computer-aided molecular engineering can assist the design of novel and highly efficient compounds for absorptive CO_2 removal.

Conflicts of interest

The authors declare no conflict of interest.

Acknowledgments

We thank the Max Planck Society for the Advancement of Science for financial support. This work is part of the Collaborative Research Centre "Integrated Chemical Processes in Liquid Multiphase Systems" (TR63, project A4) supported by the Deutsche Forschungsgemeinschaft. The research was also supported by the ERDF (European Regional Development Fund) of the Saxony-Anhalt within the 'Research Center Dynamic Systems' (CDS).

Supporting Information

Additional data about solvent densities, simulation box dimensions and CO_2 diffusion coefficients at various temperatures for aqueous aklanolamine solutions; SDFs of water and CO_2 in the vicinity of MPA and DEAB as well as RDFs for MEA are given in the Supplementary Information.

References

(1) Raupach, M. R.; Marland, G.; Ciais, P.; Le Quere, C.; Canadell, J. G.; Klepper, G.; Field, C. B. Global and Regional Drivers of Accelerating CO_2 Emissions. *Proc. Nat. Acad. Sci.* **2007**, *104*, 10288–10293.

(2) Speight, J. G. *Handbook of Natural Gas Analysis*; Johna Wiley & Sons: Hoboken, 2018.

(3) Chen, X. Y.; Vinh-Thang, H.; Ramirez, A. A.; Rodrigue, D.; Kaliaguine, S. Membrane Gas Separation Technologies for Biogas Upgrading. *RSC Adv.* **2015**, *5*, 24399–24448.

(4) Rochelle, G. T. Amine Scrubbing for CO_2 Capture. *Science* **2009**, *325* (5948), 1652–1654.

(5) Dutcher, B.; Fan, M.; Russell, A. G. Amine-Based CO_2 capture Technology Development from the Beginning of 2013-A Review. *ACS Appl. Mater. Interfaces* **2015**, *7*, 2137–2148.

(6) D'Alessandro, D. M.; Smit, B.; Long, J. R. Carbon Dioxide Capture: Prospects for New Materials. *Angew. Chem., Inter. Ed.* **2010**, *49* (35), 6058–6082.

(7) Stowe, H. M.; Hwang, G. S. Fundamental Understanding of CO_2 Capture and Regeneration in Aqueous Amines from First-Principles Studies: Recent Progress and Remaining Challenges. *Ind. Eng. Chem. Res.* **2017**, *56*, 6887−6899.

(8) Yang, X.; Rees, R. J.; Conway, W.; Puxty, G.; Yang, Q.; Winkler, D. A. Computational Modeling and Simulation of CO_2 Capture by Aqueous Amines. *Chem. Rev.* **2017**, *117*, 9524−9593.

(9) Papadopoulos, A. I.; Badr, S.; Chremos, A.; Forte, E.; Zarogiannis, T.; Seferlis, P.; Papadokonstantakis, S.; Galindo, A.; Jackson, G.; Adjiman, C. S. Computer-Aided Molecular Design and Selection of CO_2 Capture Solvents Based on Thermodynamics, Reactivity and Sustainability. *Mol. Syst. Des. Eng.* **2016**, *1*, 313–334.

(10) Monteiro, J. G. M. S.; Svendsen, H. F. The N_2O Analogy in the CO_2 Capture Context: Literature Review and Thermodynamic Modelling Considerations. *Chem. Eng. Sci.* **2015**, *126*, 455–470.

(11) Chen, Q.; Balaji, S. P.; Ramdin, M.; Gutiérrez-Sevillano, J. J.; Bardow, A.; Goetheer, E.; Vlugt, T. J. H. Validation of the CO_2/N_2O Analogy Using Molecular Simulation. *Ind. Eng. Chem. Res.* **2014**, *53*, 18081–18090.

(12) Da Silva, E. F.; Kuznetsova, T.; Kvamme, B.; Merz, K. M. Molecular Dynamics Study of Ethanolamine as a Pure Liquid and in Aqueous Solution. *J. Phys. Chem. B* **2007**, *111* (14), 3695–3703.

(13) Huang, I. S.; Li, J. J.; Tsai, M. K. Solvation Dynamics of CO_2(g) by Monoethanolamine at the Gas-Liquid Interface: A Molecular Mechanics Approach. *Molecules* **2017**, *22*, 8.

(14) Moosavi, F.; Abdollahi, F.; Razmkhah, M. Carbon Dioxide in Monoethanolamine: Interaction and Its Effect on Structural and Dynamic Properties by Molecular Dynamics Simulation. *Int. J. Greenhouse Gas Control* **2015**.

(15) Yu, Y. S.; Lu, H. F.; Wang, G. X.; Zhang, Z. X.; Rudolph, V. Characterizing the Transport Properties of Multiamine Solutions for CO_2 Capture by Molecular Dynamics Simulation. *J. Chem. Eng. Data* **2013**.

(16) Jhon, Y. H.; Shim, J.-G.; Kim, J. H.; Lee, J. H.; Jang, K. R.; Kim, J. Nucleophilicity and Accessibility Calculations of Alkanolamines: Applications to Carbon Dioxide Absorption Reactions. *J. Phys. Chem. A* **2010**, *114*, 12907–12913.

(17) Stowe, H. M.; Vilčiauskas, L.; Paek, E.; Hwang, G. S. On the Origin of Preferred Bicarbonate Production from Carbon Dioxide (CO_2) Capture in Aqueous 2-Amino-2-Methyl-1-Propanol (AMP). *Phys. Chem. Chem. Phys.* **2015**, *17*, 29184--29192.

(18) Narimani, M.; Amjad-Iranagh, S.; Modarress, H. Performance of Tertiary Amines as the Absorbents for CO2 capture: Quantum Mechanics and Molecular Dynamics Studies. *J. Nat. Gas Sci. Eng.* **2017**, *47*, 154–166.

(19) Jorgensen, W. L.; Maxwell, D. S.; Tirado-Rives, J. Development and Testing of the OPLS All-Atom Force Field on Conformational Energetics and Properties of Organic Liquids. *J. Am. Chem. Soc.* **1996**, *118*, 11225−11236.

(20) Berendsen, H. J. C.; Grigera, J. R.; Straatsma, T. P. The Missing Term in Effective Pair Potentials. *J. Phys. Chem.* **1987**, *91*, 6269−6271.

(21) Potoff, J. J.; Siepmann, J. I. Vapor–liquid Equilibria of Mixtures Containing Alkanes, Carbon Dioxide, and Nitrogen. *AIChE J.* **2001**, *47*, 1676−1682.

(22) Melnikov, S. M.; Stein, M. Molecular Dynamics Study of the Solution Structure, Clustering, and Diffusion of Four Aqueous Alkanolamines. *J. Phys. Chem. B* **2018**, *122* (10), 2769–2778.

(23) Abraham, M. J.; Murtola, T.; Schulz, R.; Páll, S.; Smith, J. C.; Hess, B.; Lindah, E. Gromacs: High Performance Molecular Simulations through Multi-Level Parallelism from Laptops to Supercomputers. *SoftwareX* **2015**, *1–2*, 19–25.

(24) Berendsen, H. J. C.; Postma, J. P. M.; Van Gunsteren, W. F.; Dinola, A.; Haak, J. R. Molecular Dynamics with Coupling to an External Bath. *J. Phys. Chem.* **1984**, *81*, 3684−3690.

(25) Nosé, S. A Unified Formulation of the Constant Temperature Molecular Dynamics Methods. *J. Chem. Phys.* **1984**, *81*, 511−519.

(26) Hoover, W. G. Canonical Dynamics: Equilibrium Phase-Space Distributions. *Phys. Rev. A* **1985**, *31*, 1695−1697.

(27) Brehm, M.; Kirchner, B. TRAVIS - A Free Analyzer and Visualizer for Monte Carlo and Molecular Dynamics Trajectories. *J. Chem. Inf. Model.* **2011**, *51*, 2007–2023.

(28) Melnikov, S. M.; Höltzel, A.; Seidel-Morgenstern, A.; Tallarek, U. A Molecular Dynamics View on Hydrophilic Interaction Chromatography with Polar-Bonded Phases: Properties of the Water-Rich Layer at a Silica Surface Modified with Diol-Functionalized Alkyl Chains. *J. Phys. Chem. C* **2016**, *120* (24), 13126−13138.

(29) Weiland, R. H.; Dingman, J. C.; Cronin, D. B.; Browning, G. J. Density and Viscosity of Some Partially Carbonated Aqueous Alkanolamine Solutions and Their Blends. *J. Chem. Eng. Data* **1998**, *43*, 378–382.

(30) Reitmeier, R. E.; Sivertz, V.; Tartar, H. V. Some Properties of Monoethanolamine and Its Aqueous Solutions. *J. Am. Chem. Soc.* **1940**, *62*, 1943–1944.

(31) Han, J.; Jin, J.; Eimer, D. A.; Melaaen, M. C. Density of Water (1) + Monoethanolamine (2) + CO_2(3) from (298.15 to 413.15) K and Surface Tension of Water (1) + Monoethanolamine (2) from (303.15 to 333.15) K. *J. Chem. Eng. Data* **2012**, *57*, 1095–1103.

(32) Snijder, E. D.; te Riele, M. J. M.; Versteeg, G. F.; van Swaaij, W. P. M. Diffusion Coefficients of Several Aqueous Alkanolamine Solutions. *J. Chem. Eng. Data* **1993**, *38*, 475−480.

(33) Idris, Z.; Eimer, D. A. Density Measurements of Unloaded and CO2-Loaded 3-Amino-1-Propanol Solutions at Temperatures (293.15 to 353.15) K. *J. Chem. Eng. Data* **2016**, *61*, 173−181.

(34) Álvarez, E.; Gómez-Díaz, D.; La Rubia, M. D.; Navaza, J. M. Densities and Viscosities of Aqueous Ternary Mixtures of 2-(Methylamino)Ethanol and 2-(Ethylamino)Ethanol with Diethanolamine, Triethanolamine, N-Methyldiethanolamine, or 2-Amino-1-Methyl-1-Propanol from 298.15 to 323.15 K. *J. Chem. Eng. Data* **2006**, *51*, 955−962.

(35) Luo, X.; Su, L.; Gao, H.; Wu, X.; Idem, R. O.; Tontiwachwuthikul, P.; Liang, Z. Density, Viscosity, and N2O Solubility of Aqueous 2-(Methylamino)Ethanol Solution. *J. Chem. Eng. Data* **2017**, *62*, 129−140.

(36) Pouryousefi, F.; Idem, R.; Supap, T.; Tontiwachwuthikul, P. Artificial Neural Networks for Accurate Prediction of Physical Properties of Aqueous Quaternary Systems of Carbon Dioxide (CO_2)-Loaded 4-(Diethylamino)-2-Butanol and Methyldiethanolamine Blended with Monoethanolamine. *Ind. Eng. Chem. Res.* **2016**, *55*, 11614−11621.

(37) Maiti, A.; Bourcier, W. L.; Aines, R. D. Atomistic Modeling of CO_2 Capture in Primary and Tertiary Amines - Heat of Absorption and Density Changes. *Chem. Phys. Lett.* **2011**, *509*, 25–28.

(38) Frenkel, D.; Smit, B. *Understanding Molecular Simulation: From Algorithms to Applications*; Academic Press: San Diego, 2002.

(39) Kusalik, P. G.; Svishchev, I. M. The Spatial Structure in Liquid Water. *Science* **1994**, *265*, 1219–1221.

(40) Ying, J.; Eimer, D. A. Measurements and Correlations of Diffusivities of Nitrous Oxide and Carbon Dioxide in Monoethanolamine + Water by Laminar Liquid Jet. *Ind. Eng. Chem. Res.* **2012**, *51*, 16517−16524.

(41) Li, M.-H.; Lai, M. D. Solubility and Diffusivity of N_2O and CO_2 in (Monoethanolamine + N-Methyldiethanolamine + Water) and in (Monoethanolamine + 2-Amino-2-Methyl-1-Propanol + Water). *J. Chem. Eng. Data* **1995**, *40*, 486–492.

(42) Mandal, B. P.; Kundu, M.; Bandyopadhyay, S. S. Physical Solubility and Diffusivity of N_2O and CO_2 into Aqueous Solutions of (2-Amino-2-Methyl-1-Propanol + Monoethanolamine) and (N -Methyldiethanolamine + Monoethanolamine). *J. Chem. Eng. Data* **2005**, *50*, 352–358.

(43) Sema, T.; Edali, M.; Naami, A.; Idem, R.; Tontiwachwuthikul, P. Solubility and Diffusivity of N_2O in Aqueous 4-(Diethylamino)-2-Butanol Solutions for Use in Postcombustion CO_2 Capture. *Ind. Eng. Chem. Res.* **2012**, *51*, 925–930.

(44) Shi, H.; Sema, T.; Naami, A.; Liang, Z.; Idem, R.; Tontiwachwuthikul, P. 13C NMR Spectroscopy of a Novel Amine Species in the DEAB-CO_2-H_2O System: VLE Model. *Ind. Eng. Chem. Res.* **2012**, *51*, 8608–8615.

(45) Maneeintr, K.; Idem, R. O.; Tontiwachwuthikul, P.; Wee, A. G. H. Synthesis, Solubilities, and Cyclic Capacities of Amino Alcohols for CO2 Capture from Flue Gas Streams. *Energy Procedia* **2009**, *1*, 1327–1334.

TOC

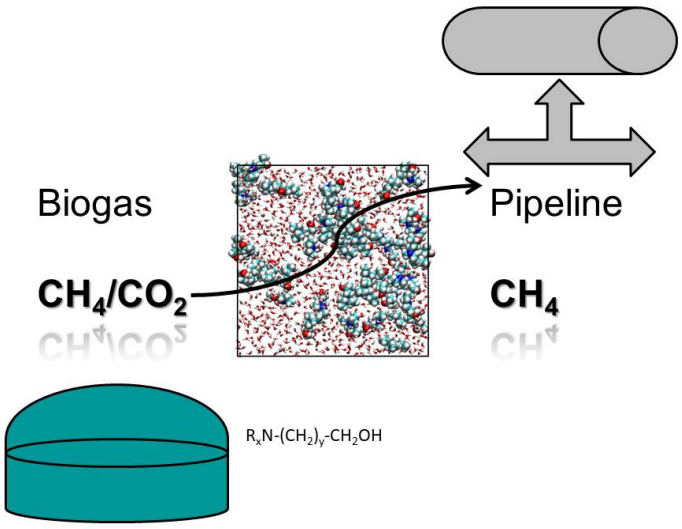

Synopsis

Biogas upgrading by absorptive sequestration of carbon dioxide displays large differences between different types of compounds at the molecular level.

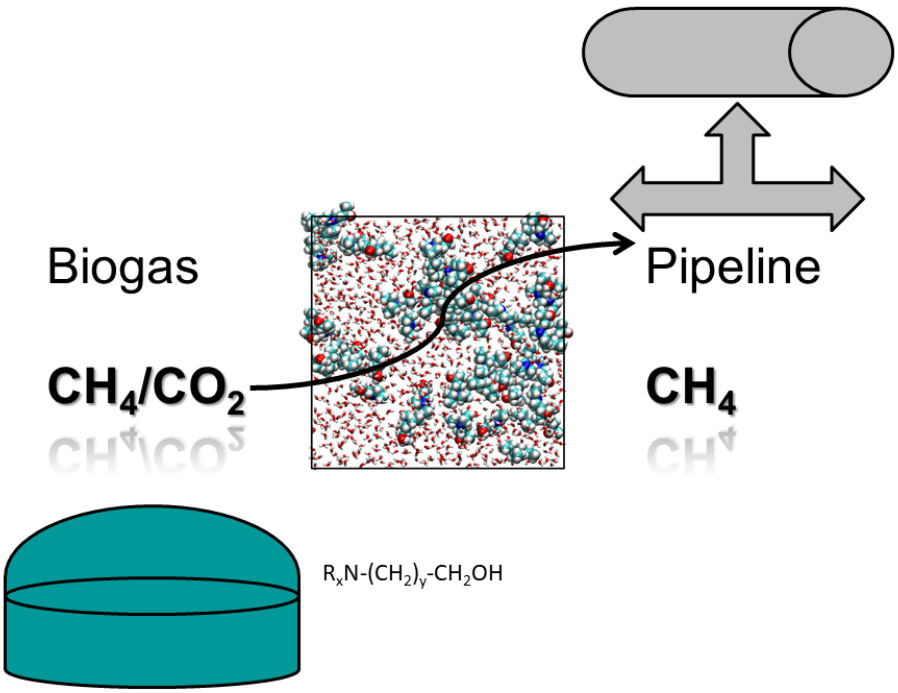

Table of Contents Entry

254x190mm (96 x 96 DPI)

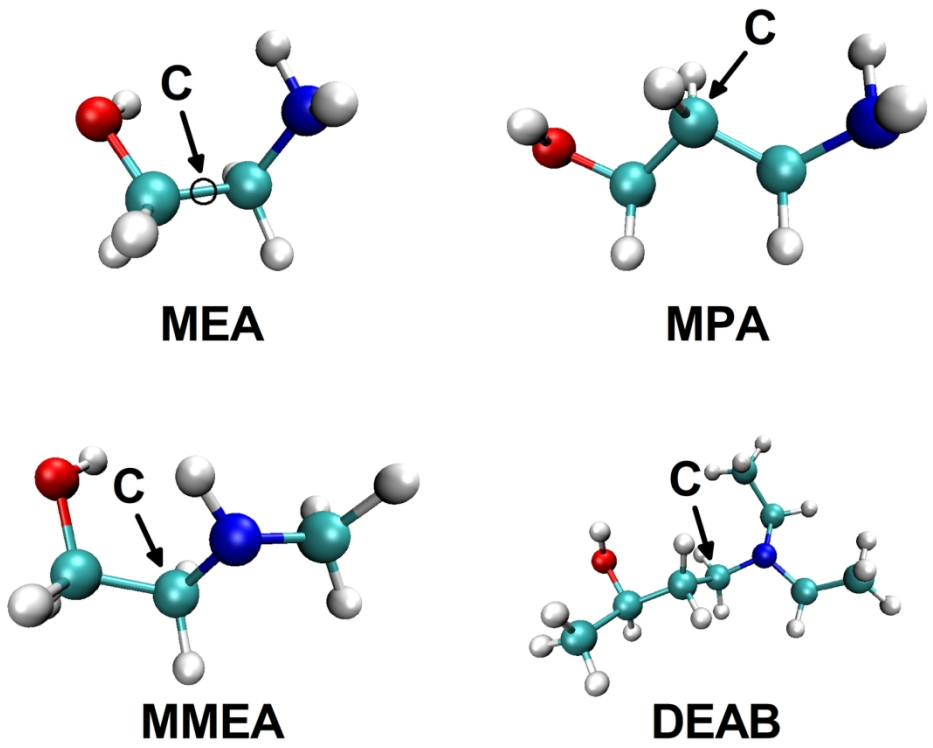

Four high-performance and sustainable alkanolamine compounds for CO2 sequestration from biogas in their low energy conformation in aqueous solution. MEA (monoethanolamine) was used as a standard and reference compound and compared with another primary amine 3-aminopropanol (MPA), a secondary amine 2-methylaminoethanol (MMEA) and a tertiary amine 4-diethylamino-2-butanol (DEAB) as to their properties in ternary mixtures with CO2 and water. The marked spot is used to analyze the liquid structure of complex mixtures by means of the radial density functions (RDFs).

79x61mm (600 x 600 DPI)

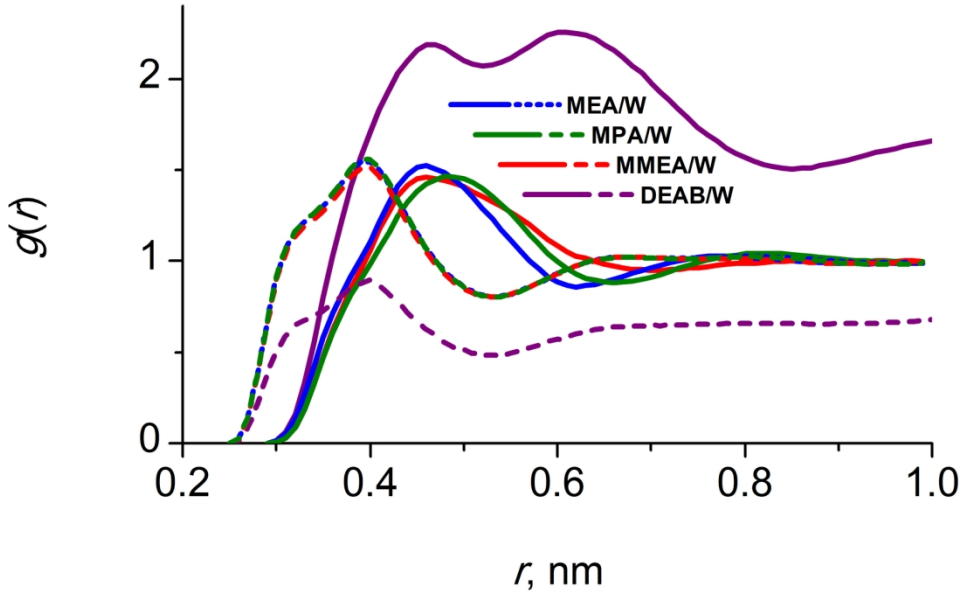

Liquid structures of ternary mixtures of CO2/water/alkanolamine. RDFs of CCO2-Calkanolamines (solid curves) and CCO2-OW (dotted and dashed curves) for the 30/70 (w/w) solution composition of alkanolamine/water at T = 313K. Blue, green, red and purples colors designate MEA, MPA, MMEA and DEAB compounds.

79x49mm (600 x 600 DPI)

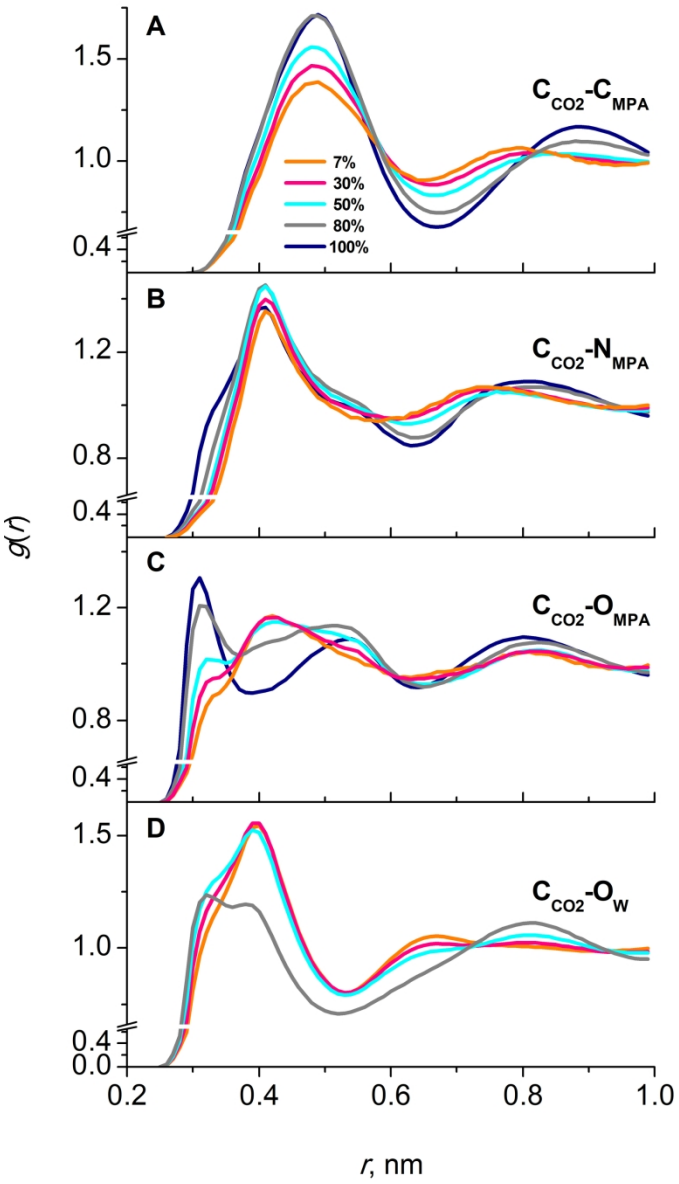

Further liquid structure details of the ternary mixture of CO2/water/alkanolamine. Results are shown here for MPA (for MEA and MMEA they can be found in the Supporting Information). Selected RDFs between carbon dioxide and MPA and water at ratios of MPA/water (w/w) of 7.5/92.5 (orange curve), 30/70 (pink), 50/50 (cyan), 80/20 (gray), and 100/0 (navy).

79x135mm (600 x 600 DPI)

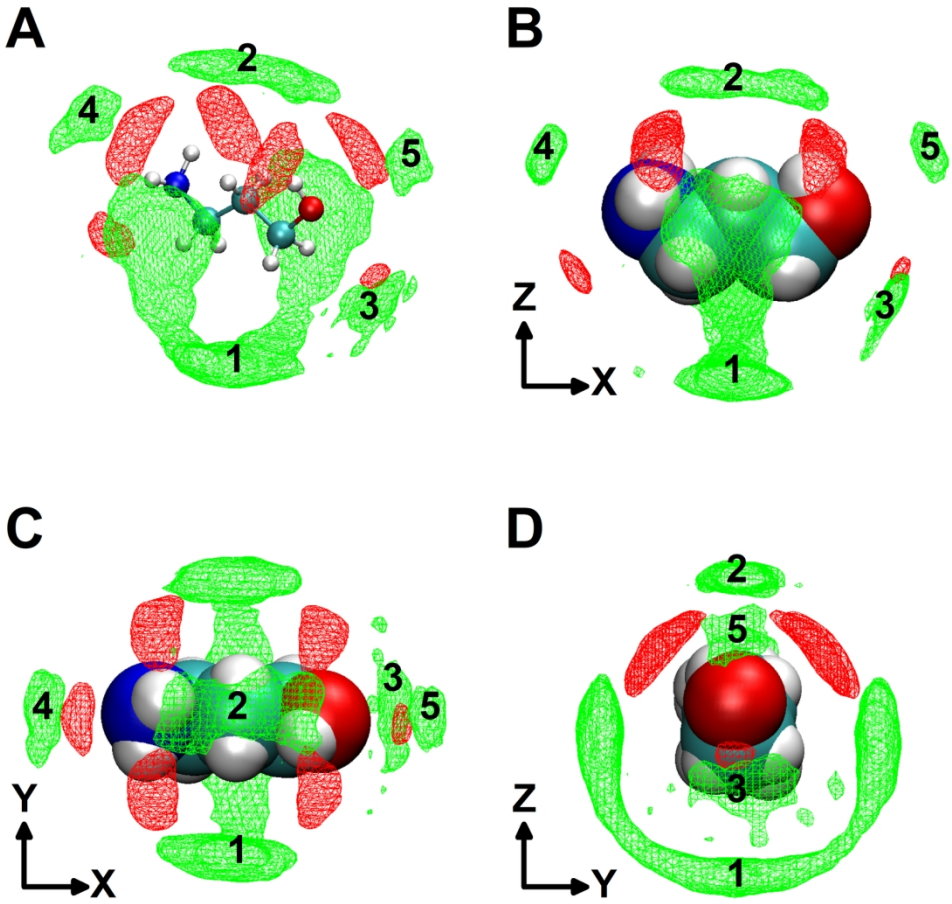

Preferential localization of CO2 (green) and water (red) molecules in vicinity of MPA. 2D projections of the spatial distribution functions (SDFs) of carbon atoms of carbon dioxide (green color) and oxygen atoms of water (red color) around MPA molecule at a 30/70 (w/w) MPA/water composition. Iso-surfaces are drawn at a density level of 50%. The five main localizations of carbon dioxide around MPA molecule are numbered (see text for a discussion). Water molecules are located mainly in three distinct regions around the rotating the amine and hydroxyl groups of MPA with which they can form hydrogen bonds and act either as an acceptor or a donor.

79x79mm (600 x 600 DPI)

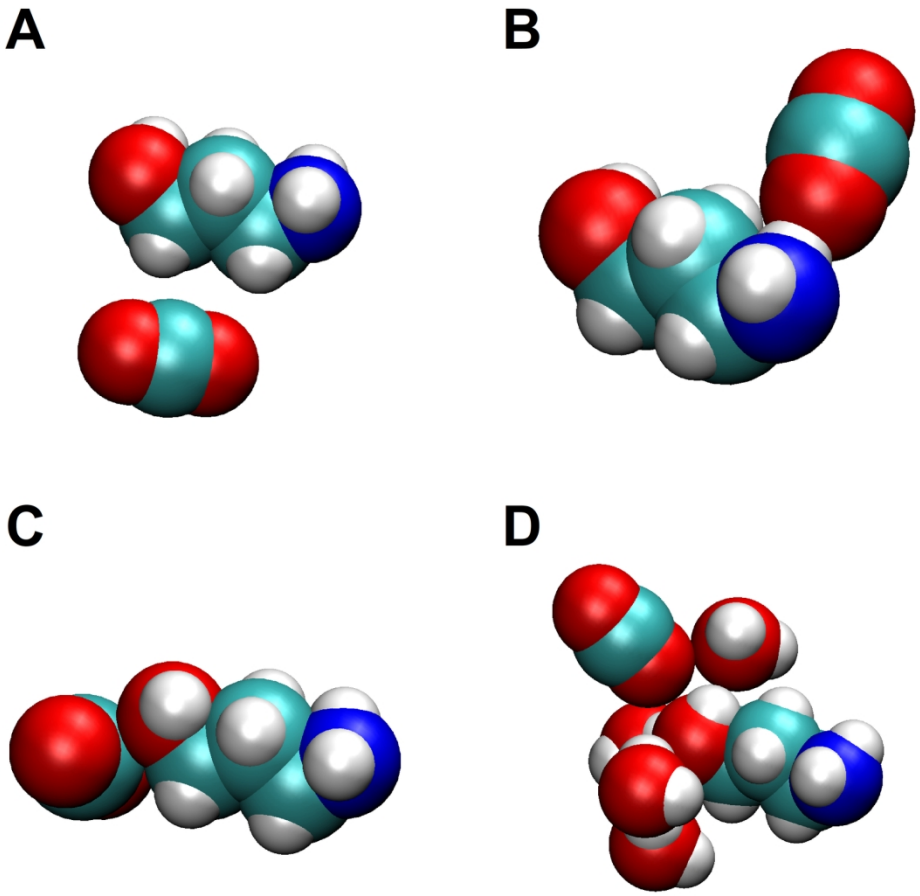

Characteristic snapshots from MD simulations showing the most relevant orientations of the first solvation shell of carbon dioxide molecules in the vicinity of the MPA molecule.

79x79mm (600 x 600 DPI)

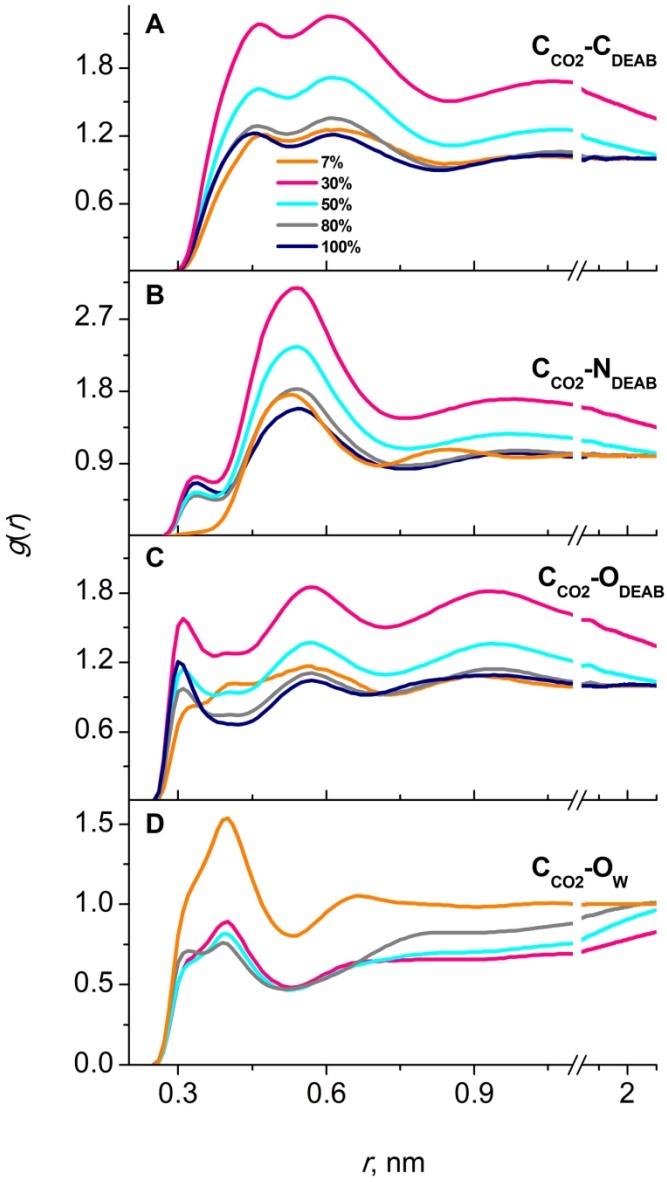

Complex liquid structure of ternary mixtures of CO2/water/DEAB at different solvent compositions. The RDFs of intermolecular interactions of carbon dioxide, DEAB and water at ratios of DEAB/water (w/w) of 7.5/92.5 (orange curve), 30/70 (pink), 50/50 (cyan), 80/20 (gray), and 100/0 (navy).

79x135mm (600 x 600 DPI)

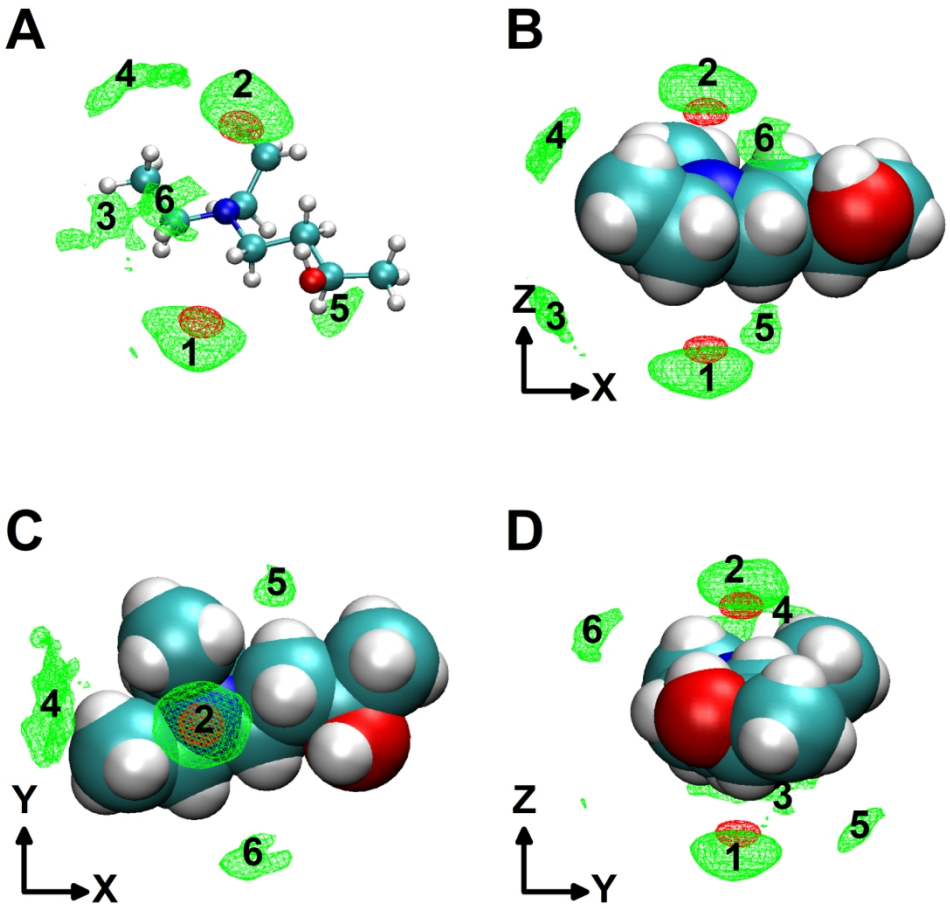

Structural mapping of the preferential localization of first solvation shell carbon dioxide (green) and water (red) molecules with respect to DEAB. The spatial distribution functions (SDFs) of carbon atoms of CO2 and oxygen atoms of water around a DEAB molecule are shown at the 30/70 (w/w) DEAB/water composition. The main chain carbon atoms are used to define the coordinate system. Iso-surfaces are drawn at 50%. The dominant five locations of carbon dioxide around the DEAB molecule are numbered (see text). Water molecule positions are shown for only two major sites of interaction close to the amine nitrogen of DEAB to which they form hydrogen bonds. Water interaction with the hydroxyl group are less prominent cannot structurally be mapped.

79x79mm (600 x 600 DPI)

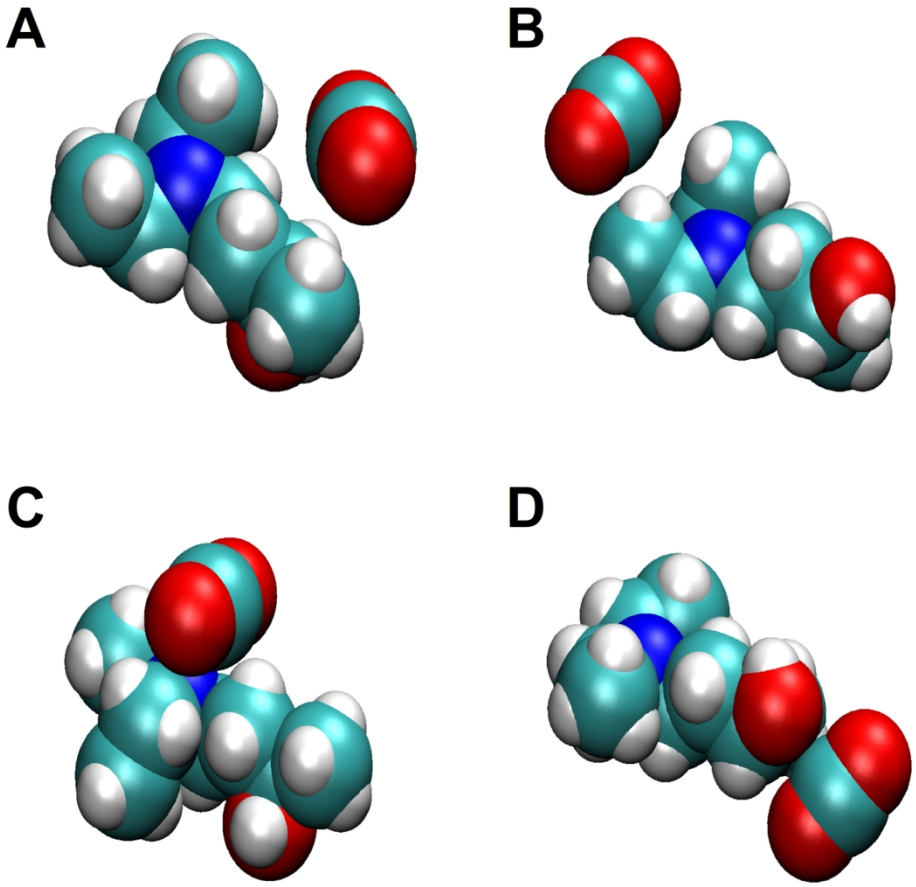

Representative snapshots from MD simulations showing the dominant association channels of carbon dioxide approaching DEAB molecule.

79x79mm (600 x 600 DPI)

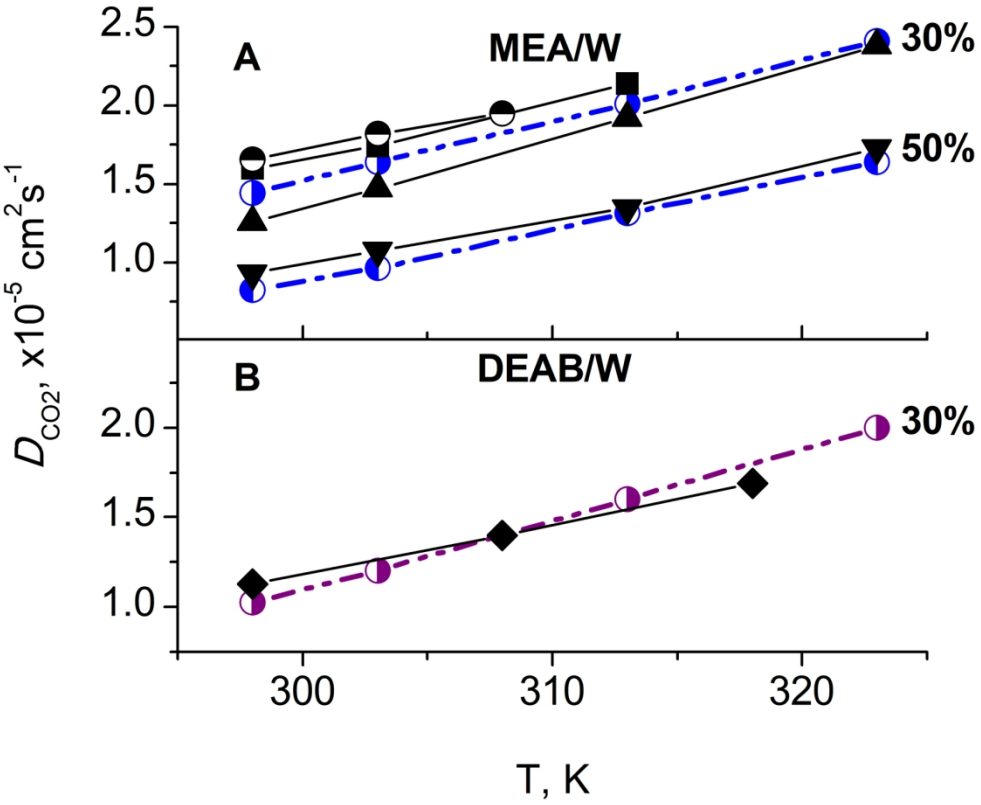

Comparison of experimental and simulated diffusion coefficients of carbon dioxide in aqueous alkanolamine solutions. Black symbols are experimental data from various sources and were derived from nitrous oxide diffusion[40-43]. The colored symbols (semi-filled blue and purple) are computed diffusion coefficients for aqueous MEA and DEAB solutions. The weight fraction composition of alkanolamine solutions in water is given.

79x64mm (600 x 600 DPI)

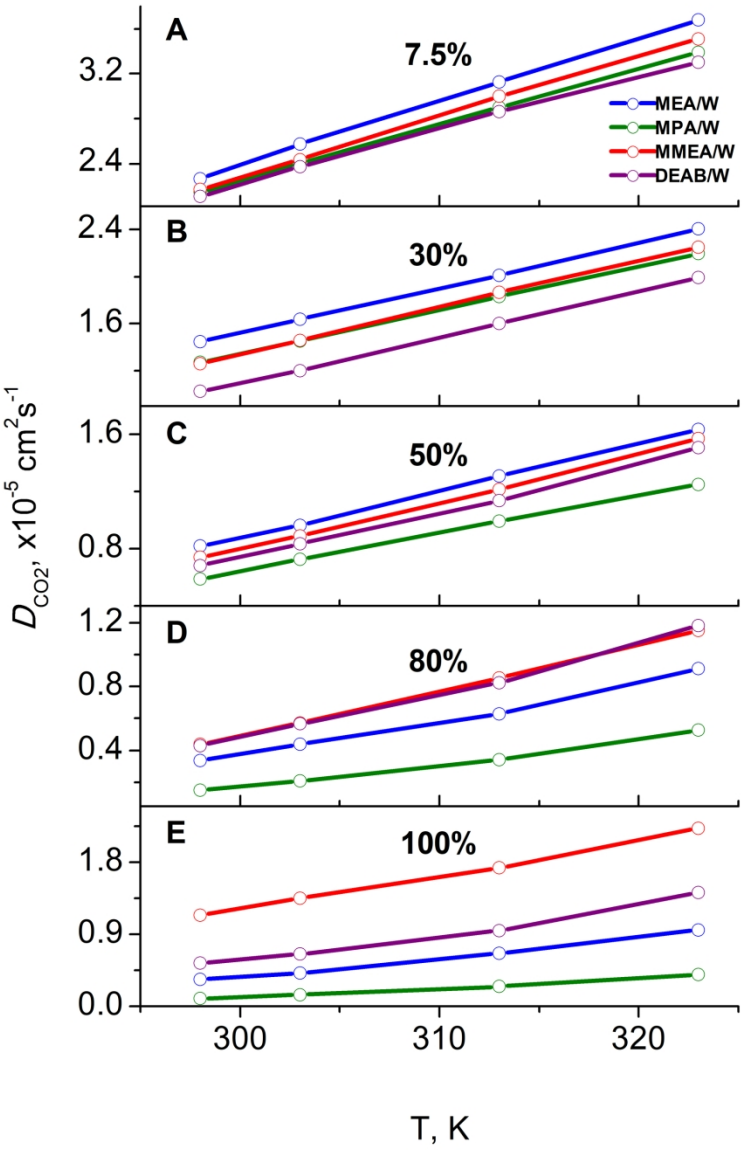

Temperature dependence of carbon dioxide diffusion coefficients in aqueous alkanolamine solutions at various mixture compositions: MEA (blue color), MPA (green), MMEA (red), and DEAB (purple). The numerical values can be found in the Supporting Information.

79x119mm (600 x 600 DPI)

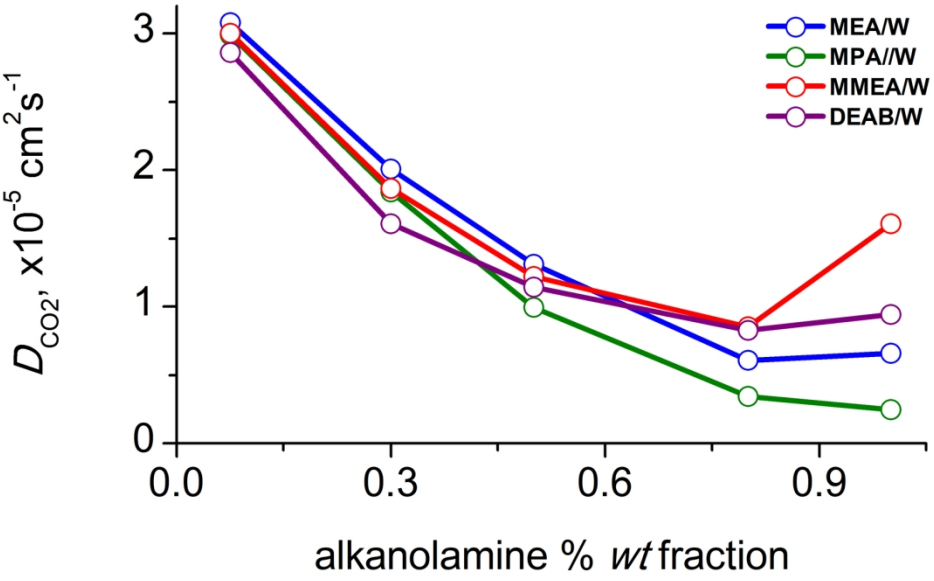

Simulated diffusion coefficients of carbon dioxide in aqueous alkanolamines over the complete range of mixture compositions at a given temperature of T= 313 K.

79x49mm (600 x 600 DPI)

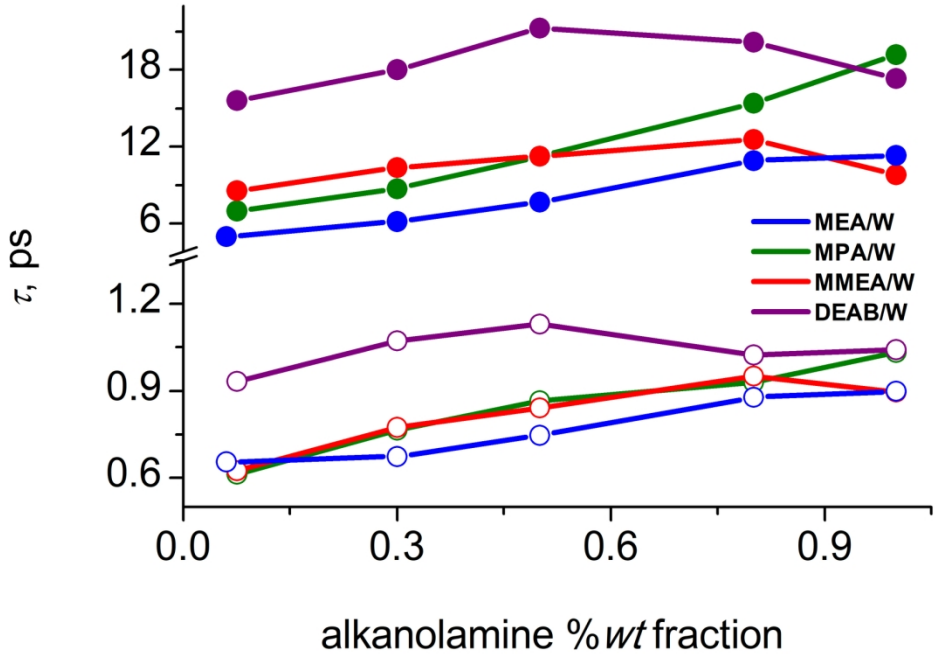

Residence times of CO2 molecules located next to alkanolamine molecules at T= 313 K. A two-component kinetics of interactions can be seen (see text for details).

79x54mm (600 x 600 DPI)